



## Introduction

On the first of August I took over the ISOLDE leadership from Yorick Blumenfeld in the middle of the most intense period of experiments ever at ISOLDE. Yorick's main legacy is the increase of visibility of the facility at CERN management level. He pursued the initialization or revitalization of agreements with other nuclear physics facilities. The ISOLDE community was enlarged with the membership of India which signed in April 2012. I am very glad to be here and serve the community and the facility after nearly thirty years of doing experiments at ISOLDE. To take over the tasks of the group leader is not easy and I would like to thank Yorick for his help and the invaluable assistance of Jenny Weterings and Magda Kowalska. I would like to thank all of them for their time and advice that have allowed me to efficiently enter the system. In November we got a third fellow for ISOLDE, Monika Stachura and from the 1<sup>st</sup> of April she coordinates the life science activities and participates in the MEDICIS project lead by Thierry Stora. In view of the shutdown I faced a few pending tasks that have been successfully achieved. The identification of modules in loan from the electronic-pool was effectively completed thanks to the help of Jan Kurcewicz. The renewal of building 115 was pending for a while and building 507 was showing significant signs of deterioration. The funds for the renewal of buildings 115 and 507 were obtained from different CERN sources. This fortunate coincidence allows us to plan a combined new building serving the full community and leaving enough space for an easy access to the future TSR building.

The year 2012 has been a great one for ISOLDE with a record 37 weeks of beam time for physics and with more protons than ever hitting the targets. Several new

techniques succeeded for the first time and various new devices were completed at ISOLDE and successfully took data. One of the greatest achievements was to implant spin-polarized  $^{31}\text{Mg}$  nuclei, at the COLLAPS setup, into a liquid medium and obtain an asymmetry beta-NMR signal. This proof of principle experiment, a novelty worldwide, bears great promises for biologically important studies of metal ion interactions with proteins and nucleic acids. In the quest for purer beams, the Laser Ion Source and Trap device (LIST) aimed to reduce surface ionization of unwanted isobars. The improved version used in 2012 resulted in an average suppression of contaminants by a factor of a thousand. An important breakthrough was achieved with the Collinear Resonance Ionization Spectroscopy (CRIS). The setup employs laser radiation to excite and resonantly ionize atomic beams using hyperfine spectroscopy and significantly reduces the background. The improved overall efficiency of 1% has allowed measurement of the hyperfine interaction of neutron deficient and neutron rich francium isotopes. Another achievement was the tilted-foil polarisation of lithium ions at REX-ISOLDE. Previously spin-oriented nuclear ensembles have been produced at COLLAPS, NICOLE and the High-Voltage Platform but this is the first time when the tilted foil approach was used with a post-accelerated beam. The degree of polarization was monitored by the beta-NMR resonance and reached 3.6 (3) %. As result of these successful experiments, three in-house students got enough data to finish their Ph.D. work.

A multi-reflection time-of-flight mass separator (MR-TOF MS) installed recently at ISOLTRAP for isobaric purification, received large coverage both in the CERN bulletin and in the CERN Courier. The ions trapped between electrostatic mirrors travel distances comparable to the LHC

circumference with reduced losses until isobar separation is achieved. It allows precision mass measurements of nuclides with ms half-lives and minute production rates. These developments have led to the successful determination of the mass of  $^{54}\text{Ca}$  and  $^{82}\text{Zn}$ .

In 2012 ISOLDE hosted new users and experimental setups. The French active target MAYA from GANIL was used to study the resonant nucleus  $^{13}\text{Be}$ . The Polish optical time-projection chamber was applied to investigate the beta-delayed deuteron emission of  $^6\text{He}$  at low energies, while resonant scattering experiments were performed with the Swedish scattering chamber.

For the first time an ISOLDE experiment was discussed in a newspaper even before taking data. This was the case for the first direct study of the astrophysically important  $^{44}\text{Ti}(\alpha, p)^{47}\text{V}$  reaction. The amount of  $^{44}\text{Ti}$  ejected in the core collapse of a supernova depends on the explosion mechanism. Due to the extension of physics program until December 17<sup>th</sup> and thanks to the effort of the coordinator and the target group, the experiment was squeezed into the ISOLDE schedule.

Details of these challenging experiments and many others are described in this newsletter; many more were discussed at the [ISOLDE workshop](#) held in December.

A new CERN website has been created, and the present one will be archived in May 2013. The ISOLDE homepage will be accessible from the new website by clicking on "about CERN" and then selecting ISOLDE from the list of experiments. We are in the process of redesigning the ISOLDE webpage following the structure and style of other CERN experiments. Jenny has almost finished creating the layout and transferring contents to the new website. After testing it will be presented to the ISOLDE collaboration committee in the July meeting.

The construction of new buildings (number 198 and 199) for HIE-ISOLDE LINAC services was completed in December. During 2012 several committee meetings took place dedicated to cost, schedule and resources of the HIE-ISOLDE project to assure that the phase 1 will be completed on schedule. The commissioning of the superconducting linac is expected to start in June 2015 and the first physics experiments in the autumn of the same year. The great interest of our community in the HIE-ISOLDE project is reflected by the fact that at the last INTC meeting 30 physics proposals, signed by 344 physicists from 81 institutes were presented.

We would like to inform you that the INTC meetings in June and October of this year will accept proposals for both HIE-ISOLDE and low energy physics while the first meeting in 2014 will be dedicated to the revision of low energy experiments.

The long shutdown period is bringing many infrastructure changes and the ISOLDE group has entered this phase effectively. It is a pleasure to work with them and it is very encouraging to feel their support and involvement. I am looking forward to seeing the realisation of these changes and the start-up of the machine again next year.

*Maria J.G. Borge*

## Information for Users:

### **Changes in user registration and dosimeter attribution**

January 1, 2013 saw changes in documents required for CERN **user registration**. The [User Registration Form](#) has changed format, but it should still be signed by the User as well as the Team Leader or Deputy (whose names are visible in CERN [Greybook](#)). The new document, which replaces the proof of employment/affiliation and proof of

insurance, is the [Home Institution Declaration](#). Just like the proof of employment/affiliation, the Declaration should be signed by the Institute's administration (HR) or management (institute Head or Director), while the team leader and deputy CANNOT sign this declaration. The first registration is now valid for up to 3 years, prolongation – up to 5 years.

On February 8, 2013 the **dosimetry service** also introduced some small changes. Users can now get access to ISOLDE with their temporary or permanent dosimeter by following a 30-minute [online course](#), which replaces the half-day RP classroom session. Users with valid dosimeters will need to follow the course only when the validity of their dosimeter expires. As before, if you don't have a medical certificate, once per calendar year you can obtain a temporary dosimeter, valid for 1 month. When presenting a medical certificate, you will obtain a permanent dosimeter valid as long as the medical certificate. It is possible for users with presence at CERN below 50% to obtain medical certificates from La Tour Hospital or local doctors, although the procedure can take a few days and has cost attached.

In case of questions or problems, contact Jenny Weterings at the ISOLDE User Support Office.

### **ISOLDE access and visits during Long Shutdown 1**

As of March 1, 2013 several changes to ISOLDE access and visits have taken place. They are mostly due to HIE-ISOLDE works and will be valid at least during Long Shutdown 1 (LS1), i.e. until June 2014.

**The ISOLDE hall extension will not be accessible to users or visitors.** This means that access from the front (i.e. from the main entrance side) is no longer

permitted and one should enter from the Jura side. If you need to move equipment, check beforehand with Erwin Siesling.

In addition, ISOLDE **users** are required to wear **safety helmets and safety shoes** when they ENTER the hall. You can bring the safety shoes from your institute or buy them in CERN stores. Several safety helmets should be provided by your ISOLDE experiment – they will not be provided by the ISOLDE group.

ISOLDE **visits** are still allowed, but with access via the Jura side of the hall and limited to two groups of 12 visitors at once. As before, you need to inform somebody from the local physics group about the intention of a visit (until September 2013: Jan Kurcewicz, then again me). All visitors need to wear safety helmets that are provided by the in-house group. Note that these helmets are reserved for visitors, not users. Visit itineraries during LS1 EXCLUDE the hall extension.

### **ISOLDE Document and Photo Collection in CERN Document Server**

This February the CERN library launched an [ISOLDE Collection](#) on the CERN Document Server ([CDS](#)). The Collection groups together various ISOLDE documents existing in CDS: articles found in InSpire, CERN theses, CERN Notes, INTC documents, and even ISOLDE photos.

The Photo Collection now includes several dozen photos of ISOLDE taken in 2013. We will soon add captions to them.

To increase the visibility of your research and of ISOLDE, **we'd like to ask you to [submit to CDS](#) the many missing theses based on ISOLDE data.** In a few months we should also have a DOI-based system allowing you to add your ISOLDE articles to the ISOLDE articles Collection.

Please let me know if you spot some bugs in the Collection or if you have problems adding your documents or photos.

*Magdalena Kowalska*

## 2013 HIE ISOLDE work in the hall

Even though 2013 will be a year of no physics at ISOLDE it does not mean it will be quiet in the experimental hall, on the contrary! The installation works for HIE ISOLDE have already set off and will continue through the year far into 2014. The HIE ISOLDE work in the hall for this year will mainly involve civil engineering in the form of cutting of existing walls, digging trenches and construction of the extension to the shielding tunnel.

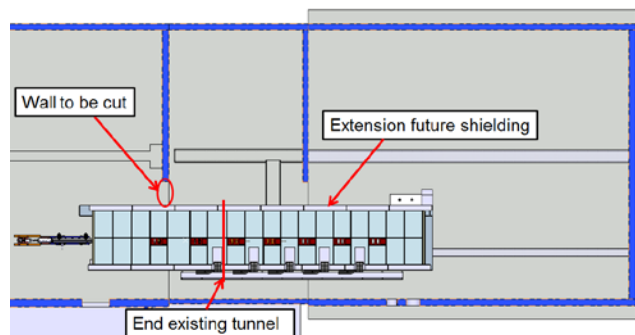


**Fig. 1:** Civil Engineering for HIE ISOLDE in the hall in 2013.

It also involves the installation of new cooling and ventilation systems, modification of the platform to house future HIE ISOLDE power supplies and equipment and installation of the infrastructure such as cable trays and tubing for the new linac and the High Energy Beamlines.

The preparations already started in December with the removal of equipment and experiments in the hall extension. For the Miniball structure, the scattering chamber and the beta-NMR setup and some of their delicate equipment we did not want to transport, we have allocated dedicated storage space in the hall that is convenient

both for the users as well as the HIE ISOLDE work that needs to be carried out.

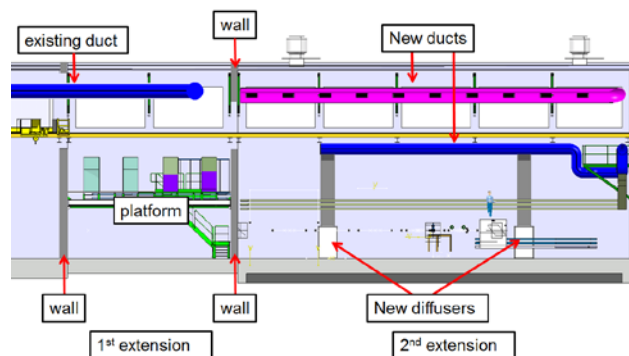


**Fig. 2:** New cooling and ventilation systems, and modification of the equipment platform

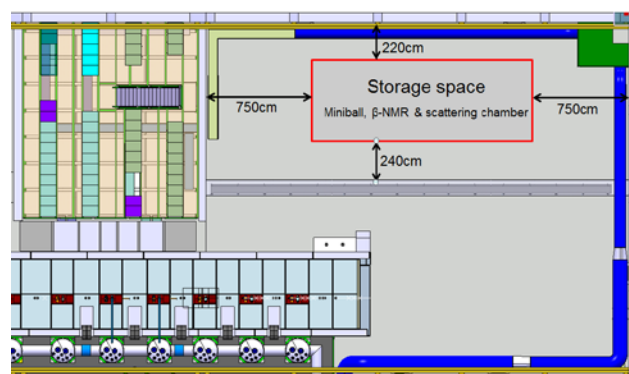


**Fig. 3:** Dedicated storage space in the hall extension for delicate and hard to move equipment

The REX linac was running until mid-February for HIE ISOLDE beam instrumentation tests. As soon as the machine stopped the water was cut and the dismantling of the existing REX beamlines started.

Demineralized cooling water will not be available to the facility until the summer due to modifications on the existing water station for HIE ISOLDE. Power cuts are not to be expected. In case there are perturbations they will be communicated well in advance to the user community.

Main message to the users for 2013: Avoid the extension of the ISOLDE experimental hall and the tunnel area. Use the entrance to ISOLDE from the Jura side and apply all

safety rules (helmet and safety shoes). Hazards will be noise, dust and the handling of heavy weights. All necessary precautions will be taken by the workers to minimize the dust (cutting will be done with water to have no, or little, dust particles in the air). Coordination for the users goes through Magda Kowalska and Marek Pfützner, for HIE ISOLDE through Erwin Siesling.

*Erwin Siesling on behalf of the HIE integration team*

## Experiment reports:

### **IS370: Shape determination of $^{72}\text{Kr}$ and low-spin structure study of $^{72}\text{Br}$ via the beta decay of $^{72}\text{Kr}$**

The  $N=Z$  nucleus  $^{72}\text{Kr}$  is situated in the mass region  $A\sim 70-80$ , where phenomena such as shape coexistence [1,2,3] and possibly also  $np$  pairing effects can show up. From the astrophysical point of view,  $^{72}\text{Kr}$  is of great interest as it is involved in the  $rp$ -process of stellar nucleosynthesis.  $^{72}\text{Kr}$  is a waiting point nucleus because  $^{73}\text{Rb}$ , next step in the one-proton capture, is unbound and there is a competition between the two-proton capture and the beta decay of  $^{72}\text{Kr}$ . For this reason, a good knowledge on its beta decay properties such as  $B(\text{GT})$  distribution are of vital importance for astrophysical calculations. From the nuclear structure point of view,  $^{72}\text{Kr}$  is an interesting case of an exotic  $N=Z$  nucleus whose shape (in g.s.) has been predicted oblate [4] and can be inferred by means of beta decay studies as it is described below.



*Fig. 1: Picture of the "Lucrecia" Total Absorption Spectrometer located in the ISOLDE hall and used in the IS370 experiment for the study of the  $^{72}\text{Kr}$  beta decay described in this article.*

Previous results from IS370 and IS398 experiments on neighbour nuclei using the Total Absorption Spectroscopy (TAS) technique with the "Lucrecia" detector shown in fig. 1, have delivered successful results providing information on the shapes of the ground state of the  $^{76}\text{Sr}$  and  $^{74}\text{Kr}$  nuclei [5,6]. The procedure is based on the fact that in this region of shape coexistence mean field calculations performed using the self-consistent Hartree-Fock plus RPA method with Skyrme interactions [7] predict very different  $B(\text{GT})$  distributions in the  $Q_\beta$  window for the different deformations of the ground state of the parent nucleus. By comparison of the experimental  $B(\text{GT})$  distribution and the theoretical predictions one can deduce the deformation of the ground state of the parent nucleus, in this case  $^{72}\text{Kr}$ .

A high-resolution beta-decay study of  $^{72}\text{Kr}$  was done a decade ago at ISOLDE [8], but the conversion coefficients of the de-excitation transitions were not measured and the spin-parities of the low-lying states in the daughter nucleus,  $^{72}\text{Br}$ , were only tentatively assigned. This information turned out to be crucial in order to perform the analysis of the total decay spectroscopy study provided by the TAS data.

The aim of this work was to do a complete study of this decay to determine the  $B(\text{GT})$  distribution in the full  $Q_\beta$  window. In order to obtain the required information two complementary measurements were performed within the IS370 experiment.

The low-spin structure of  $^{72}\text{Br}$  was studied by the combination of a gamma and conversion-electron detection systems. The latter system works as sketched in fig. 2, where a set of permanent magnets focuses the conversion electrons towards a  $\text{Si}(\text{Li})$  detector. A central tungsten piece prevents

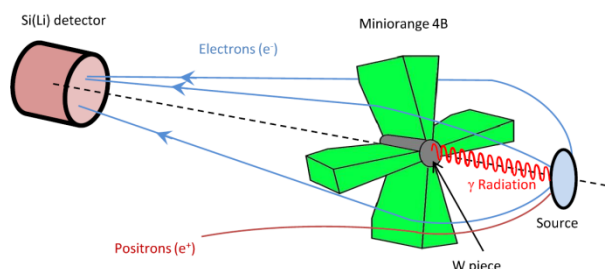


**Fig.2:** Schematic diagram of the electron spectrometer used in the IS370 experiment showing its mode of operation.

the X-ray and gamma radiation from reaching the Si(Li) detector in order to obtain clean electron spectra. From this measurement, the experimental conversion coefficients for 10 low-energy transitions in the de-excitation of  $^{72}\text{Br}$  were obtained and their dominant multipolarities determined. The latter were useful to determine the spin and parity of the levels involved in the transition. In addition they are needed to extract the B(GT) distribution in the TAS data analysis.

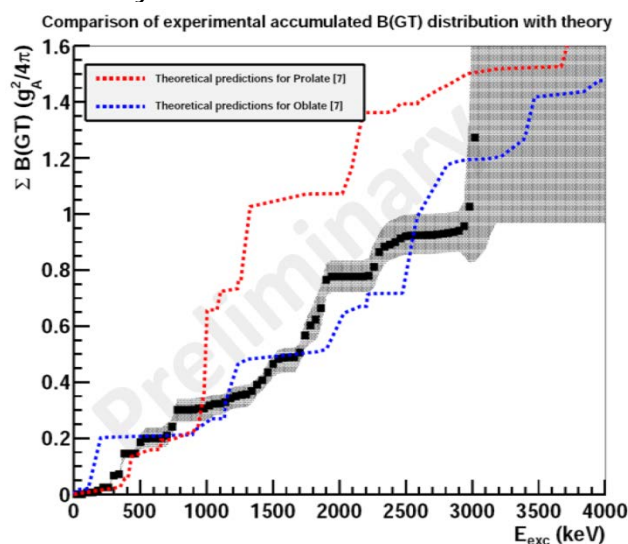


**Fig.3:** The preliminary B(GT) distribution of the beta decay of  $^{72}\text{Kr}$  obtained from the analysis of the TAS data is compared with the theoretical predictions for prolate and oblate deformations from ref. [7].

The beta feeding in the full  $Q_\beta$  window was extracted from the TAS data and the B(GT) distribution obtained. The comparison of the

experimental B(GT) distribution with the theoretical predictions for the different deformations is shown in fig. 3. This comparison suggests oblate deformation for the ground state of  $^{72}\text{Kr}$ . Our results can be compared with and will be complementary to the coulomb excitation experiment of  $^{72}\text{Kr}$  also performed at ISOLDE (IS478) and described later in this issue.

- [1] K. Heyde and J.L. Wood, Rev. Mod. Phys. 83, 1467 (2011).
- [2] J.H. Hamilton et al., Phys. Rev. Lett. 32, 239 (1974).
- [3] C. Chandler et al., Phys. Rev. C 56, R2924 (1997).
- [4] W. Nazarewicz et al., Nucl. Phys. A435, 397 (1985).
- [5] E. Nácher et al., Phys. Rev. Lett. 92, 232501 (2004).
- [6] E. Poirier et al., Phys. Rev. C 69, 034307 (2004).
- [7] P. Sarriguren et al., Nucl. Phys. A658, 13 (1999) and Nucl. Phys. A691, 631 (2001).
- [8] I. Piqueras et al., Eur. Phys. J. A 16, 313 (2003).

*J. A. Briz (for the IS370 Collaboration)*

### IS433: New DAQ for WITCH to push systematic uncertainties on $a$ for $^{35}\text{Ar}$

Last year was a very exciting one for fundamental physics at CERN with the discovery of a new boson at the LHC. Searches for new physics at CERN are also performed in low energy experiments, by studying the weak interaction processes in nuclear decays. At ISOLDE the WITCH experiment has been set up for measurements of the  $\beta$ - $\nu$  angular correlation coefficient  $a$  for the primary candidate  $^{35}\text{Ar}$ . A deviation from the value predicted by the Standard Model would hint at the presence of new physics not currently incorporated into the standard theory.

The WITCH experiment [1,2] uses the 30 keV ion beam which has been cooled and bunched by REXTRAP. The  $\mu\text{s}$ -short pulses are transported through the horizontal beam line towards the pulsed drift tube (PDT), which decelerates the ion ensemble before it is captured in the buffer-gas-filled cooler trap, the first of the WITCH Penning traps. Here the ions are cooled to an energy distribution width of below an eV to reduce the systematic effect of thermal energy broadening, which should be as small as possible after the transfer of the ions to the second Penning trap, the decay trap. The decay trap is under UHV to avoid charge exchange reactions of the singly charged noble gas ions  $^{35}\text{Ar}^+$  as well as scattering of the recoil ions ( $^{35}\text{Cl}^{n+}$ ), which constitute the signal. The chlorine ions are guided first along the magnetic field lines over the magnetic field gradient to the analysis plane, where their total energy is analysed with a retardation potential. The measurements at WITCH thus constitute ion intensity as a function of the applied retardation potential.

The online experiments in 2011 [3] showed that the WITCH experiment can be operated for the purpose it has been designed for, as mentioned in last year's newsletter. Nevertheless, during the data analysis it was found that the position-sensitive branch of the data acquisition was too slow to account for the detection inhomogeneity over the surface of the main detector. As a remedy a prototype DAQ, developed by the ICT engineers at LPC Caen, was implemented. This FASTER system is an 8 channel fast ADC with a few 10 ns time resolution, which can handle an average data rate of up to 100 kHz. In addition the collected charges from the delay lines and the main signal (capacitively decoupled from the front plate of the MCP detector) are written to the data stream. For synchronization purposes one channel

has been dedicated to time stamp the REXTRAP trigger. As a check of the synchronization the voltage applied on the spectrometer electrodes has been fed via a voltage divider to one of the channels and is part of the data stream for all registered events.

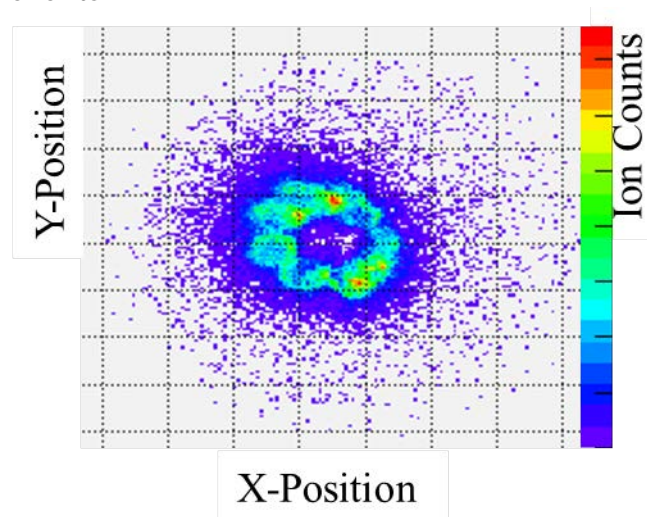


*Fig.1: Position distribution of events after ejection of the ions from the decay trap. 10 different phases distributed over 1 magnetron period are integrated.*

This new data acquisition allows correcting for a potential inhomogeneity in the detection efficiency via a calibration measurement as a function of MCP surface coordinates. Furthermore, due to the high count rate the DAQ can accept, ion ensembles ejected from the traps which reach the detector within some  $100\mu\text{s}$  will be registered above the background level. In Fig. 1 an example of a test measurement is shown, where the magnetron motion of the ions in the decay trap has been integrated for 10 phases. Here ions are kept in the decay trap, and the time before ejection is varied in 3 ms steps, while the magnetron period is about 32 ms. The large circle represents the magnetron motion with the small ones being the projections of the ion ensemble with one specific phase. The scale of the position depends highly on the applied voltages in the spectrometer and

reacceleration section, and is thus qualitative only. These dependencies are important inputs for simulations [4,5] as a cross check of the WITCH electrical and magnetic fields.

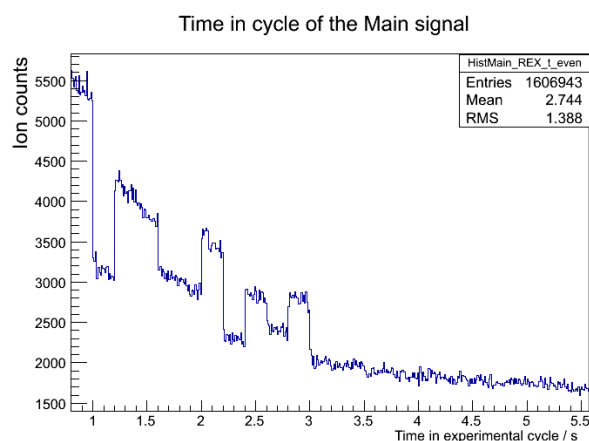


**Fig.2:** Raw data for a single half-hour run taken in November 2012 with the WITCH experiment. Ion intensity is plotted as a function of time in the experimental cycle. Before 0.8s the traps are loaded from REXTRAP. The variation in intensity is due to the application of different retardation potentials throughout the cycle, while the  $^{35}\text{Ar}$  sample in the decay trap is decaying. At 3.2 s the remaining ions are ejected (away from the detector) and the background being monitored.

This new equipment, together with a better understanding of the detector itself [6], is one of the key achievements to push not only the statistical but also the systematic uncertainty on the  $\beta$ - $\nu$  angular correlation coefficient  $a$  below 1%. This is required for a final, competitive result of the WITCH experiment. Throughout the long shutdown we will continue with tests for further characterization to support analysis of the online data.

One of the typical spectra acquired in the WITCH online experiment in November 2012 is shown in Fig. 2. The raw data is plotted as counts as a function of time in the experimental cycle. Since the recoil ions are escaping the trap due to the energy gained in the decay, the signal intensity is

an exponential decay partly weakened by the application of a higher retardation voltage. The data presented in Fig. 2 contain a background originating from a particle trap between the PDT and the magnetic field, which sporadically releases charges throughout the entire experimental cycle. Further analysis will take this background and other effects into account. Preliminary results are planned for end of 2013.

- [1] M. Beck et al., Nucl. Instr. Meth. A 503 (2003) 567.
- [2] V.Yu. Kozlov et al., Nucl. Instr. and Meth. B 266 (2008) 4515-4520.
- [3] S. Van Gorp, PhD thesis, IKS, KU Leuven (2012).
- [4] S. Van Gorp et al., Nucl. Instr. and Meth. A 638 (2011) 192-200.
- [5] P. Friedag, Diploma thesis, IfK, University Münster (2008).
- [6] P. Friedag, PhD thesis, IfK, University Münster (2013).

*M. Breitenfeldt (for the WITCH Collaboration)*

## IS488 and LOI88: Biophysics activities at ISOLDE

In 2012 our biophysics group carried out  $^{111}\text{Ag}$ -,  $^{111\text{m}}\text{Cd}$ , and  $^{199\text{m}}\text{Hg}$  Perturbed Angular Correlation (PAC) experiments, exploring the chemistry of heavy metal ions interacting with biomolecules, as well as  $^{31}\text{Mg}$   $\beta$ -NMR experiments on a liquid sample. These experiments were complemented by application of a variety of other spectroscopic techniques, most notably NMR, UV-Vis absorption, circular dichroism, and fluorescence spectroscopy, as well as quantum mechanical calculations of the spectroscopic properties, supporting the interpretation of the experimental data. One of the most interesting group of systems studied by us last year were the

metalloregulatory proteins of the MerR family [ref]. The MerR family are transcriptional regulators that respond to the change of intracellular metal ion concentration or availability. CueR, a member of this family shows a very sensitive and selective response for monovalent soft metal ions, e.g. Cu(I), Ag(I), Au(I) while showing no regulatory activity (in vitro) for divalent metal ions including Hg(II) and Zn(II). The high metal binding ability of these proteins inspired us to design and synthesize several oligopeptides, containing the native or slightly modified multiple Cys-containing metal binding sequences of a CueR protein. The Cd(II), Hg(II) and Ag(I) binding features of these ligands have been studied by PAC spectroscopy (besides other methods). Studies on the metal ion coordination of the short peptide ligands were aimed at the better understanding of how metal ion selection by the native proteins occurs. The linear coordination environment provided by CueR for monovalent metal ions should be more than suitable for Hg(II). Indeed, linear{2xCys-S<sup>-</sup>} type coordination have been found with all of the investigated ligands. Besides, the strong toxic metal binding ability of these molecules may have a potential in future analytical or environmental applications involving toxic metal ion capture. We are intending to extend these studies for the protein level, meaning experiments in the various metal ion – CueR protein systems and this would allow to compare the coordination environment of the metal ions within the peptides and the protein.

The year 2012 was particularly successful for the biophysics collaboration at ISOLDE because we conducted the world's first  $\beta$ -NMR experiments on liquid samples. This technique is well established in nuclear and solid state physics, but has never been used to study chemistry in solution, due to a

number of technical challenges, such as having a liquid sample in a high vacuum environment. The prototype of a biophysics  $\beta$ -NMR chamber, designed and assembled in 2010-2011, was applied in online experiments during the summer last year. The NMR resonance recorded for  $^{31}\text{Mg}$  in ionic liquid constitutes the first  $\beta$ -NMR spectrum ever recorded for a liquid sample, demonstrating the feasibility of applying  $\beta$ -NMR spectroscopy in chemistry and biology.

*L. Hemmingsen, A. Jancso and Monika Stachura on behalf of the IS488 and I88 collaborations*

### **IS453: Lattice location of $^{27}\text{Mg}$ and $^{11}\text{Be}$ in GaN and AlN**

Magnesium is currently the only feasible  $p$ -type dopant in the technologically important wide band gap semiconductors GaN and AlN. All applications of GaN involving  $p$ -junctions such as blue or white LEDs, blue lasers or high-frequency power diodes rely on Mg acceptors substituting for Ga, but so far no direct lattice location experiments were possible for Mg in any of the nitride semiconductors.

Following the realization of laser-ionized, clean  $^{27}\text{Mg}$  ( $t_{1/2}=9.45$  min) beams from Ti targets at ISOLDE we have for the first time measured its lattice location implanted into GaN and AlN using the on-line  $\beta^-$  emission channeling technique.

As was to be expected, the majority of  $^{27}\text{Mg}$  was found in substitutional sites of Ga and Al. Surprisingly, a significant fraction of Mg could also be identified close to the octahedral interstitial O sites in the RT as-implanted state. Increasing the implantation temperature to 600°C, the interstitial Mg was fully converted to substitutional Ga or Al sites (Fig. 1). Note that minority fractions of probes on interstitial O sites are not easy to detect, but evident from the clear

reduction of the planar channeling effects of the (01-10) set of planes in the as-implanted state. Our results hence represent the first direct evidence for interstitial Mg in nitride semiconductors.

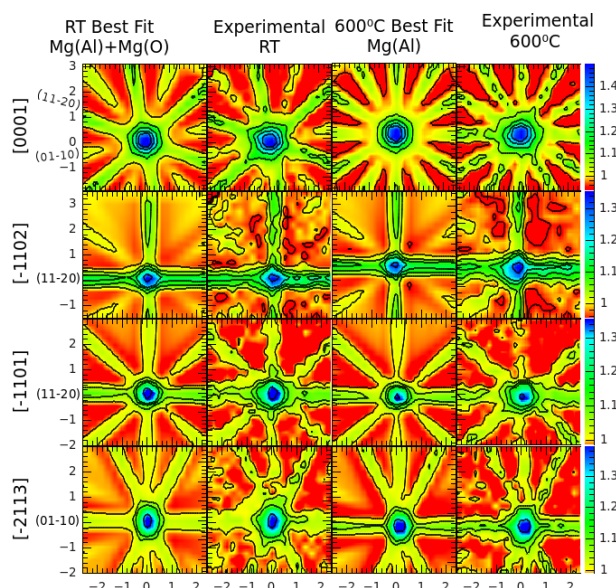


**Fig. 1:** Comparison of experimental emission channeling patterns (row 2 and 4) and best fit results (row 1 and 3) for  $^{27}\text{Mg}$  in AlN implanted at room temperature and 600°C. The RT results were best fitted by 75% of Al-site and 22% of interstitial O-site  $^{27}\text{Mg}$ , while at 600°C only Al-site Mg is left. The contribution from O-site  $^{27}\text{Mg}$  is clearly visible from the reduction of the planar (01-10) channeling in the as-implanted state.

Also during 2012 first tests were performed using the short-lived  $^{11}\text{Be}$  (13.8 s) isotope (Fig. 2), which was obtained by means of laser ionization from a Ta target.  $^{11}\text{Be}$  is a

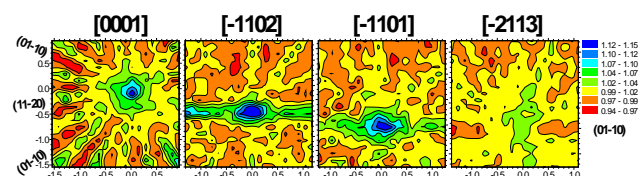


**Fig. 2:**  $\beta^-$  Emission channeling patterns from  $^{11}\text{Be}$  implanted into GaN at RT.

particularly difficult probe for emission channeling experiments due to the high

energies of the emitted  $\beta^-$  particles (endpoint 11.5 MeV), which causes a strong background of scattered electrons and in addition very narrow channeling effects, requiring to place the detector at a larger distance from the sample. While it is obvious from the patterns that the majority of  $^{11}\text{Be}$  occupies Ga sites, the observed clear blocking along (01-10) planes is also evidence for a significant fraction on interstitial O sites, similar to  $^{27}\text{Mg}$ .

*Ulrich Wahl, Lúgia Amorim and Lino Pereira  
(for the EC-SLI Collaboration)*

## IS456: First use of the LIST at ISOLDE: study of the neutron-rich polonium isotopes

The quest for beam purity has been a driving force for the target and ion source developments. The use of the RILIS has offered a great leap forward in getting 'impossible' beams and improving the selectivity of the ion source [1]. It suffers however from the surface ionized isobars, which are produced in the same cavity as the laser ions.

The Laser Ion Source and Trap (LIST) was conceived to suppress those surface-ionized isotopes [2,3]. Fig.1 shows a photograph of the device. It decouples the laser ionization from the surface ionization by a positively charged repeller electrode right after the ionizer of the target. This hinders the passage of the surface ions. Only neutral atoms may diffuse into the ion guide where they are then selectively ionized by the RILIS lasers. The LIST has been designed and developed by Mainz University and CERN and was successfully tested for the first time on-line at ISOLDE in 2011. Based on the on-line results, the LIST has been modified to improve its performance in terms of efficiency, selectivity, and reliability and extensively tested at the off-line

separators in Mainz and at ISOLDE. During the measurement campaign in 2012, the laser ionization for two elements, Mg and Po, and the suppression of various surface-ionized isotopes have been measured. Laser ionization of Mg was improved from a 50-fold (2011) to a 20-fold loss compared to normal RILIS mode. For Po, a loss-factor to RILIS of only 10 was determined. The overall suppression factor for the surface ions was measured for  $^{26,30}\text{Na}$ ,  $^{46}\text{K}$ , and  $^{205,212,220}\text{Fr}$ . Suppression factors varied from 70 in case of  $^{212}\text{Fr}$  to up to 10000 in case of  $^{26}\text{Na}$ , but were mostly of the order of 1000.



*Fig. 1: A photograph of the LIST device.*

The LIST was finally used for the production of n-rich Po beams online. For the previous campaigns of IS456, beams of  $^{216,218}\text{Po}$  had been produced in semi-offline conditions using radiogenic precursors [4], but no odd-A isotope could be approached in this way [5].

In the 2012 campaign, purified beams of  $^{216-219}\text{Po}$  were successfully produced thanks to the strong suppression of  $^{213,218-220}\text{Fr}$  and in-source laser spectroscopy was carried out on these beams. The beam purity can be seen in the alpha-decay energy spectrum (Fig.2). Only polonium isotopes and their

daughters are seen, except for some trace amounts of  $^{217}\text{Rn}$  ( $T_{1/2}=540\mu\text{s}$ ), whose origin is still under investigation.

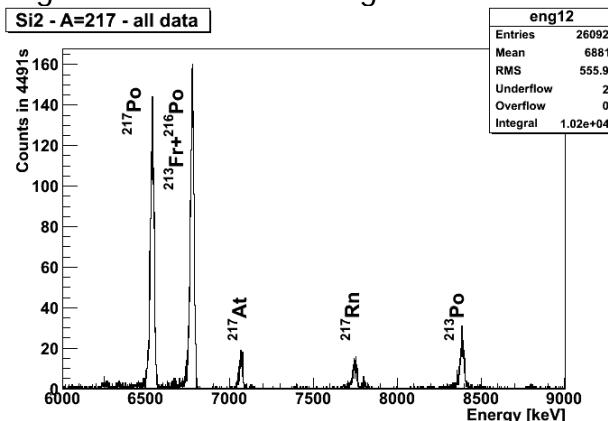


*Fig. 2: Alpha-decay energy spectrum at A=217.*

- [1] V. Mishin et al., NIMB 73:550 (1993)
- [2] K. Blaum et al., NIMB 204:331-335 (2003).
- [3] F. Schwelinius et al., Rev. Sci. Instrum. 81:02A515 (2010)
- [4] T.E. Cocolios et al., PRL 106:052503 (2011).
- [5] M.D. Seliverstov et al., PLB 719:362-366 (2013).

*Daniel Fink and Thomas Elias Cocolios for the RILIS-LIST-Windmill collaborations*

## IS466 and IS534: Investigating $\beta$ -delayed fission in the neutron-deficient lead region

Investigating the process of  $\beta$ -delayed fission ( $\beta\text{df}$ ) provides valuable experimental input towards a theoretical description of the fission process. This rare decay occurs when a precursor nucleus undergoes  $\beta$  decay to a nuclear state close to the top of the fission barrier in the daughter nucleus. This unique tool facilitates the study at low excitation energies, since the available energy for excitation is limited by the Q value of  $\beta$  decay. Its experimental study is attainable in both the well-studied uranium region, where this process was first discovered [1], and the neutron-deficient lead region. The recently observed

asymmetric mass distribution in fission fragments of  $^{180}\text{Hg}$ , following the  $\beta$  decay of  $^{180}\text{Tl}$ , triggered a systematic experimental study of the  $\beta$ df properties in the latter region studying neutron-deficient francium and astatine nuclei [2]. The experiments were conducted at the LA1 beam line of ISOLDE using the Windmill detection set-up.

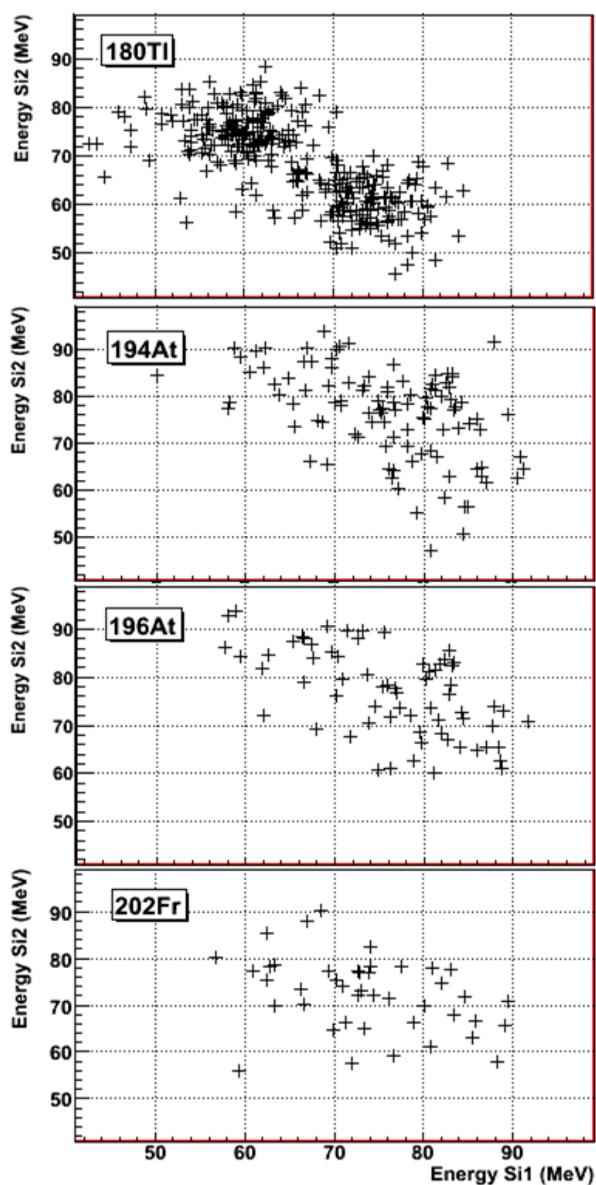


**Fig.1:** Observed fission fragment energy distributions following the  $\beta$ df of  $^{202}\text{Fr}$  and  $^{194,196}\text{At}$ , the fragments observed after  $\beta$ df of  $^{180}\text{Tl}$  are shown for comparison.

In this system pure isotopic beams produced by ISOLDE are implanted in thin

carbon foils, which are housed on a rotatable wheel. Silicon detectors placed on both sides of these foils are used to measure fission fragments as well as  $\alpha$  and  $\beta$  radiation. In addition, germanium detectors are employed to detect  $\gamma$  radiation. In the years 2011-2012,  $\beta$ -delayed fission of  $^{200,202}\text{Fr}$  (IS466) and  $^{194,196}\text{At}$  (IS534) isotopes has been firmly identified using this method. Moreover, preliminary analysis of the observed mass distributions, as deduced from the detected energy in the Si detectors (Fig. 1), show broader and more symmetric distributions as compared to the asymmetric split in the  $^{180}\text{Tl}$  case.

[1] V.I. Kuznetsov and N.K. Skobelev, *Yadernaya Fizika* 4, 279 (1966).

[2] A.N. Andreyev et al., *PRL* 105, 252502 (2010)

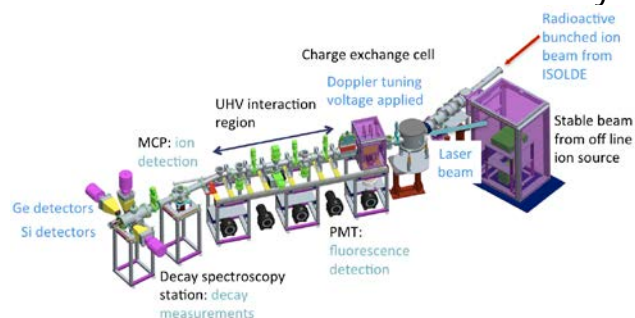
*Lars Ghys (for the Windmill Collaboration)*

## IS471: Collinear resonant ionization spectroscopy of francium isotopes

Last year, the CRIS (collinear resonant ionization spectroscopy) collaboration successfully performed new measurements on the neutron-deficient and neutron-rich francium isotopes,  $^{202-207,211,218-221,229,231}\text{Fr}$  [1]. In addition, October 2012 saw the new technique of laser assisted decay spectroscopy being performed for the first time, on the three low-lying states of  $^{204}\text{Fr}$ .

This is a continuation in the experimental campaign to study specific nuclear structure features in the francium isotopes: the possible onset of shape coexistence in neutron-deficient francium isotopes, the magnetic moment and isomer shift of the  $(\pi s_{1/2}^{-1})1/2^+$  intruders state in  $^{201,203}\text{Fr}$  and the border of the region of reflection asymmetry in  $^{218,219}\text{Fr}$ . In addition to the

information provided by hyperfine measurements, decay spectroscopy can provide detailed information about the isomeric structure of  $^{202,204}\text{Fr}$  and its decay.



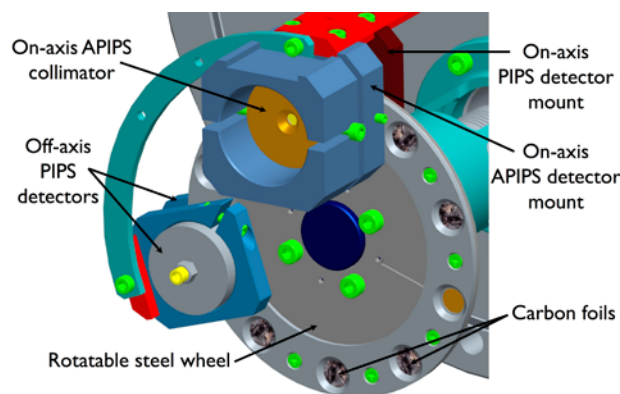
**Fig.1:** Drawing of the CRIS beam line and the decay spectroscopy station (DSS).

Fig. 1 shows the CRIS beam line [2] where laser radiation is used to step-wise excite and ionize an atomic beam using its characteristic hyperfine structure. In addition to hyperfine measurements, this technique offers the ability to purify an ion beam that is heavily contaminated with radioactive isobars, including the separation of the ground state of an isotope from its isomer [3], allowing laser assisted decay spectroscopy to be performed.

A 40 keV bunched ion beam from HRS+ISCOOL was delivered to the CRIS beam line and neutralized by a potassium vapour charge exchange cell. The neutral beam was collinearly overlapped with light from two synchronized pulsed lasers (422nm + 1064nm). The laser frequency was scanned, and the atoms were ionized when the laser light was on resonance with the 422nm atomic transition. The resonantly produced ions were deflected to the decay spectroscopy station (DSS) [4], shown in Fig. 2. Here, they were detected with an MCP, for hyperfine structure measurements, or implanted into a carbon foil for decay measurements [5]. The DSS consists of a rotating wheel implantation system with Canberra Si PIPs detectors for alpha decay spectroscopy, and two Ge detectors around the implantation site for gamma-ray

detection.

The ionization scheme for francium consisted of a resonant (422nm) step from the  $7^2S_{1/2}$  ground state to the  $8^2P_{3/2}$  excited



**Fig.2:** Drawing of DSS Windmill and newly installed Faraday Cup to aid beam tuning.

state [6], followed by a non-resonant 1064nm step into the continuum. The 422nm light was provided by the RILIS team via a fibre optic cable, and the laser frequency was scanned utilizing the new RILIS control system.

Collinear resonant ionization spectroscopy was performed on  $^{202-207,211,218-221,229,231}\text{Fr}$  and the analysis of these results is currently underway. The hyperfine structure of  $^{204}\text{Fr}$ , its ground state (blue) and isomers (green and red), can be seen in Fig. 3.

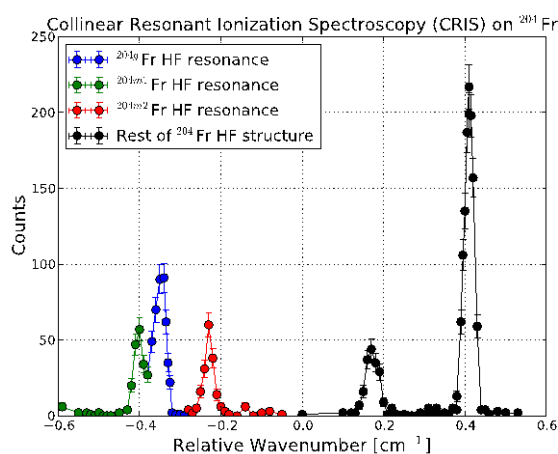


**Fig.3:** The HFS of  $^{204}\text{Fr}$  measured at CRIS.

Laser assisted decay spectroscopy was successfully performed on  $^{202,204,218}\text{Fr}$  during

the IS471 run. Fig. 4 shows the alpha spectrum that was obtained when the laser was tuned onto resonance with a transition (shown in Fig. 3.) in the hyperfine structure of the ground state (blue), first isomeric state (green) and second isomeric state (red) in  $^{204g,m1,m2}\text{Fr}$ . This demonstrates the ability of CRIS as a purification process, producing pure isomeric beams for decay spectroscopy.

This year, the total experimental efficiency of the CRIS technique was close to 1%. This value combines the neutralization efficiency, beam transmission and laser-ionization efficiencies. The figure represents an improvement of four orders of magnitude since last year, and further improvements are expected. The extremely low background in Fig. 3 is due to the low probability (about  $10^{-6}$ ) of collisional ionization. This will be further reduced by maintaining the vacuum below  $10^{-9}$  mbar.

The long shutdown will be spent making significant improvements to the CRIS beam line. The CRIS data acquisition system and the DSS DigiDAQ system will need to be fully integrated to gain full advantage of the technique. Other modifications will include improvements in the vacuum in the beam line and reduction of the collisional ionized

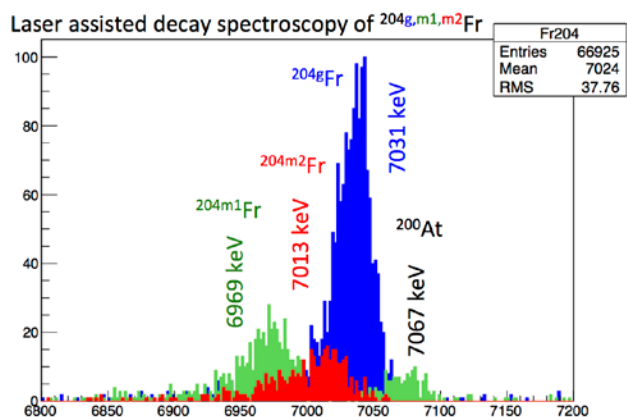


**Fig. 4:** Laser assisted decay spectroscopy of  $^{204g,m1,m2}\text{Fr}$ . Pure isomeric beams were produced using CRIS as a purification technique.

background. A new design for the DSS is currently in preparation, optimizing the gamma-ray detection efficiency for the planned experiments in 2014.

- [1] J. Billowes et al. CERN-INTC-2008-010. INTC-P-240 CERN, Geneva (2008)
- [2] T.J. Procter et al., *J. Phys.: Conf. Ser.* 381 012070 (2012)
- [3] V. Letokhov, *Opt. Commun.* 7 59 – 60 (1973)
- [4] M.M. Rajabali, K.M. Lynch, T.E. Cocolios et al., *Nucl. Instrum. Methods Phys. Res. A* 707 35 (2013)
- [5] K.M. Lynch et al., *J. Phys.: Conf. Ser.* 381 012128 (2012)
- [6] H.T. Duong et al. *Eurphys. Lett.* 3 175 (1987)

*The authors would like to thank the RILIS team and the ISOLDE technical staff for their dedicated assistance during this experimental campaign.*

*Kara M. Lynch for the CRIS Collaboration*

## IS475: Measurements of octupole collectivity in $^{220,222}\text{Rn}$ and $^{222,224}\text{Ra}$ using Coulomb excitation

A Coulomb excitation experiment was carried out between 31<sup>st</sup> August and 2<sup>nd</sup> September 2012 using the highly efficient gamma-ray detector array MINIBALL. A beam of around  $5 \times 10^3$   $^{221}\text{Rn}$  ions/second accelerated to 2.85 MeV/u was delivered to the MINIBALL array, and impinged on a  $^{120}\text{Sn}$  (2.0 mg/cm<sup>2</sup>) target for around 30 hours.

Although there was a relatively low beam current, correlations made between the particles detected in the CD detector and gamma-rays detected in MINIBALL allow an event-by-event Doppler correction and a random background subtraction, leading to a very clean spectrum that can be seen in figure 1. The initial beam current was lower than anticipated; however, three clear

gamma-ray peaks can be identified at 201.0, 223.5, and 289.3 KeV.

Work is on-going with regards to analysis of the spectrum. It is of interest to note the large number of x-rays, which would be expected in this nucleus, as there are highly converted transitions, adding to the normal counts from atomic processes.

A new silicon detector, SPEDE, for conversion electron measurements will be installed at HIE-ISOLDE. This device will enhance the experimental set-up to include simultaneous conversion electron and gamma-ray spectroscopy. Analysis of this odd mass nucleus will give quantitative information about the octupole correlations, with implications on the search for permanent atomic electric dipole moments.

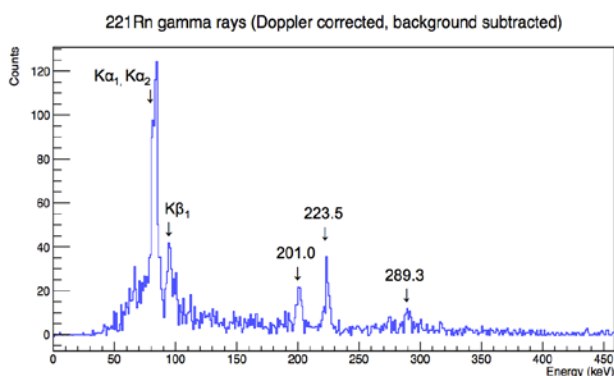


**Fig.1:** Prompt gamma-ray spectrum following Coulomb excitation of  $^{221}\text{Rn}$  projectile at 2.85 MeV/u on a  $^{120}\text{Sn}$  target (2 mg/cm<sup>2</sup>), Doppler corrected for radon (background subtracted).

The original proposal for the experiment can be found at

<http://cdsweb.cern.ch/record/1100218/files/INTC-P-244.pdf>.

*George O'Neill (for the MINIBALL Collaboration)*

## IS478: Shape determination in Coulomb excitation of $^{72}\text{Kr}$

Unlike prolate deformed nuclei, the oblate ones are rare across the nuclear landscape [1]. Consequently, very limited data exist and the underlying mechanism responsible for the emergence of oblate deformation in nuclei is not well understood. In the A~70 region of shape co-existence [2], the first excited  $2^+$  state in  $^{72}\text{Kr}$  is a special case because all the existing experimental and theoretical information indicate an oblate deformation for this state [3,4]. However, no direct experimental evidence has been found to date to confirm these expectations (see the contribution on page 6. of this newsletter).

In an attempt to obtain the sign of the spectroscopic quadrupole moment, utilizing the re-orientation effect [5] (c.f. Fig.1), and thereby to determine the shape of  $^{72}\text{Kr}$  residing in this state, we initiated a low-energy inelastic Coulomb excitation study of  $^{72}\text{Kr}$  using a beam produced at REX-ISOLDE. After extensive efforts from the target group to develop the beam [6] and several attempts using Miniball to study  $^{72}\text{Kr}$  using Coulomb excitation, in May 2012 we successfully collected the first data. The 2.85 MeV/u beam was used to bombard a  $^{104}\text{Pd}$  target of 2 mg/cm<sup>2</sup> thickness and the  $\gamma$  rays were detected using the Miniball setup. The  $\gamma$ -ray yield (~150 counts) seen in Fig.2 for the  $2^+ \rightarrow 0^+$  transition in  $^{72}\text{Kr}$  is comparable to that seen in the work presented in Ref.[5], which in turn suggests that the sign of the spectroscopic quadrupole moment can be obtained. The analysis is currently in progress.

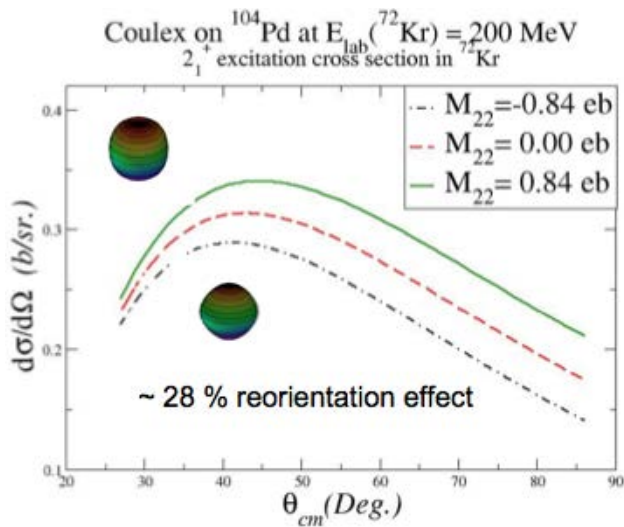


**Fig.1:** The population of the  $2^+$  state is different (by 28 %) if it is oblate (green/solid line) or prolate (black/dash-dotted) shape. This should be reflected in the  $\gamma$ -ray yield (see Fig.2).

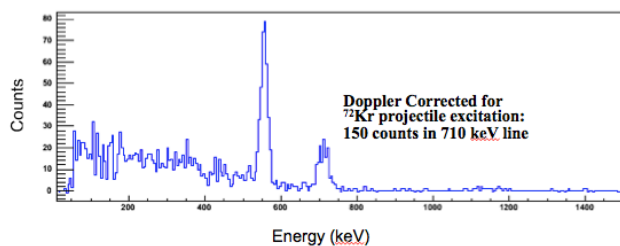


**Fig.2:** The Miniball  $\gamma$ -ray spectrum gated on the target as well as beam particles detected in the CD detector placed inside the target chamber.

- [1] P. Möller et al., At. Data Nucl. Data Tables, 59, 185 (1995).
- [2] K. Heyde and J. L. Wood, Rev. Mod. Phys. 83, 1467 (2011).
- [3] A. Gade et al., Phys. Rev. Lett. 95, 022502 (2005).
- [4] E. Bouchez et al., Phys. Rev. Lett. 90, 082502 (2003).
- [5] A. M. Hurst et al., Phys. Rev. Lett. 98, 072501 (2007).
- [6] B.S. Nara Singh et al. CERN-INTC-2008-042 / INTC-CLL-004, 06/10/2008

*B.S. Nara Singh for the IS478 collaboration*

## IS484 and IS529: Ground-state properties of $^{51}\text{K}$ and $^{49-52}\text{Ca}$ isotopes from laser spectroscopy

With the measurement of the hyperfine spectra of  $^{51}\text{K}$  in 2012, the potassium campaign (IS484) was successfully completed. As a continuation of our exploration of this region, last year we began measurements on Ca (IS529). By combining bunched beam laser spectroscopy with our new highly efficient optical detection station, the signal-to-background ratio was significantly improved, allowing  $^{51}\text{K}$  to be studied with only 4000 ions/s.

Since four peaks are observed in the hyperfine spectrum in Figure 1, a nuclear spin of  $1/2$  was excluded. The spin was determined by comparing experimental magnetic moments assuming different spins

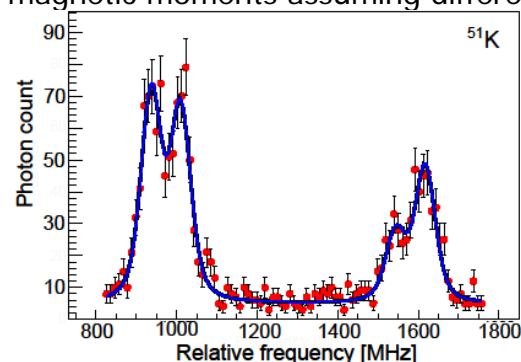


**Fig. 1:** A typical hyperfine spectrum of  $^{51}\text{K}$ . The solid line is a fit to the data.

to Shell Model calculations and  $I = 3/2$  was established for  $^{51}\text{K}$  [1]. The magnetic moment is a good probe for investigating the composition of the ground-state wave function. For  $^{51}\text{K}$ , the dominant component is a hole in proton  $1d_{3/2}$  which points to the re-inversion of the proton single-particle levels  $2s_{1/2}$  and  $1d_{3/2}$ .

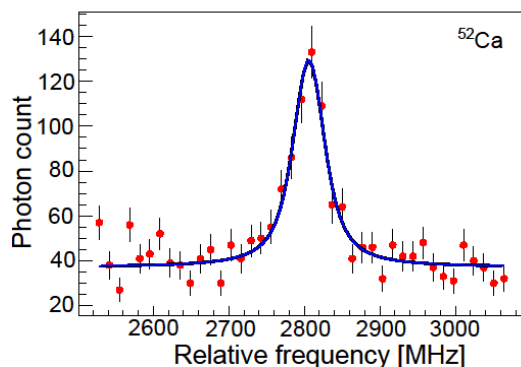


**Fig. 2:** A spectrum of  $^{52}\text{Ca}$  recorded with  $\approx 300$  ions/s. The solid line is a fit to the data.

In our Ca campaign (IS529) the isotopes up to  $N = 32$  were investigated, providing significant new nuclear structure information. The electronic transition that was studied is sensitive to both the magnetic moment and the quadrupole moment of the odd-Ca isotopes. A spectrum of  $^{52}\text{Ca}$  recorded with  $\approx 300$  ions/s is shown in Figure 2.

The mean square charge radii  $\langle r^2 \rangle$  in this region have been found to show a surprising transition. Below  $N = 28$  a substantial  $Z$ -dependence was observed whilst above, a monotonic increase with very little influence by the number of protons was found. The origins of this transition will be explored in a future publication.

In order to reach the  $^{53,54}\text{Ca}$  isotopes, significant development work of a non-optical detection technique is being undertaken during the CERN shutdown period.

[1] J. Papuga et al., PRL 110(2013)172503

*J. Papuga on behalf of the COLLAPS Collaboration*

## IS486: The next generation of implantation chambers for GPS

Currently two chambers for the GLM branch of ISOLDE are being constructed. The first chamber will replace the current collection chamber and provide a load-lock system for sample exchange. The second chamber allows for beam deceleration and post-acceleration thus providing collections with an extended energy range reaching from virtually 0 keV to 120 keV for a primary beam energy of 60 keV.

The new sample transport system allows for collections into tilted samples and improved radiation protection since the samples are easier accessible and can be changed more quickly.

The deceleration chamber is mounted behind the implantation chamber and both chambers can be used alternately thus providing optimal beam time usage.



**Fig.1:** CAD drawing of both chambers in the GLM cave. The schematic blue structure in the back is a dummy of the ISOLDE beam line. The big chamber on the right side is the new implantation chamber while the smaller chamber on the left side is the deceleration chamber. At the exit of the deceleration chamber the valve on the left providing the possibility of shooting through both chambers and adding additional chambers is also visible.

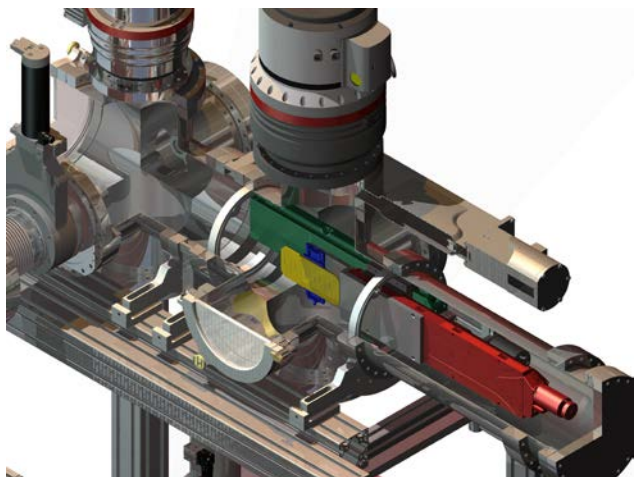


**Fig.2:** Sectional view of the sample transport system. Samples are loaded from the door in the foreground while the ISOLDE beam enters the chamber from the flange visible in the background in between the two turbo pumps

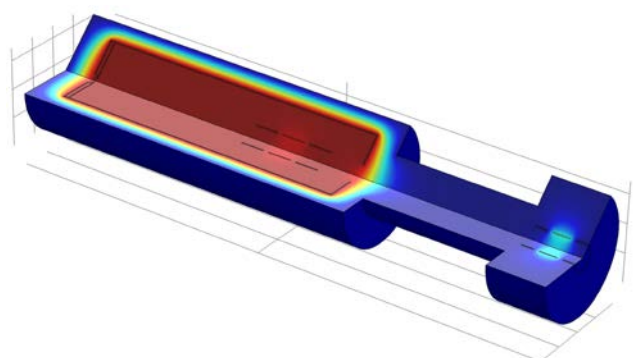


**Fig.3:** Simulation of the ion optics in the deceleration chamber. The ion beam enters from the right and is decelerated and focused using a container with selectable potential as well as two Einzel lenses

Behind the deceleration chamber additional chambers can be mounted and it is possible to use the ion optics contained in the implantation and deceleration chambers to focus the ISOLDE beam right into these chambers thus reducing the need to mount and unmount chambers in order to conduct different types of collections.

*Matthias Nagl (for the IS486 group)*

## IS487: Can Electric Field Gradients probe “spontaneous polarization” in ferroelectric compounds?

Some works can be found in the literature back to the 1960s and 1970s where the quadrupole hyperfine interaction was measured in ferroelectrics; by assuming a known nuclear quadrupole moment, the electric field gradient (EFG) tensor was the material property of interest in these works. In the absence of powerful theoretical tools, when only empirical case-to-case models could be implemented and discussed, both the EFG and the spontaneous polarization ( $P$ ), the main property in ferroelectrics, were (mis)understood from the theoretical side. Despite these facts, the hint for a relation between the EFG and  $P$  could be established in some materials. 40 years later, the conceptual framework of both of these properties has improved, and it is now possible to calculate them accurately without adjustable parameters using first principles tools. Therefore, we attempted to validate this relation in simple ferroelectrics using the *ab initio* (density functional theory) calculations. The results are unequivocal and indeed show that the EFG is linearly proportional to  $P$  squared in perovskite-type materials, matching the previous experiments and models. An additional term is needed only for very large distortion ranges, for which there are not yet experimental data available. Our computational “experiments” also allow the accurate characterization of the EFG tensor for a wide range of materials, which established a linear relationship between the EFG tensor components, and a variation of EFG with the square of the atomic number at the corner site of the perovskite lattice, which is a very general relation still poorly understood.  $P$  is a difficult quantity to measure with more conventional

techniques and restricted to macroscopic, non-metallic, samples. The EFG, in contrast, can be measured in a wide range of conditions at the local atomic scale, where the distortions actually happen, which makes a deeper study of this relationship worthwhile. ISOLDE, with its large number of available Perturbed Angular Correlation probe nuclei, is the ideal place to carry experiments under extreme stress conditions to understand polarization and phase transitions in materials via the probe of the hyperfine interactions.

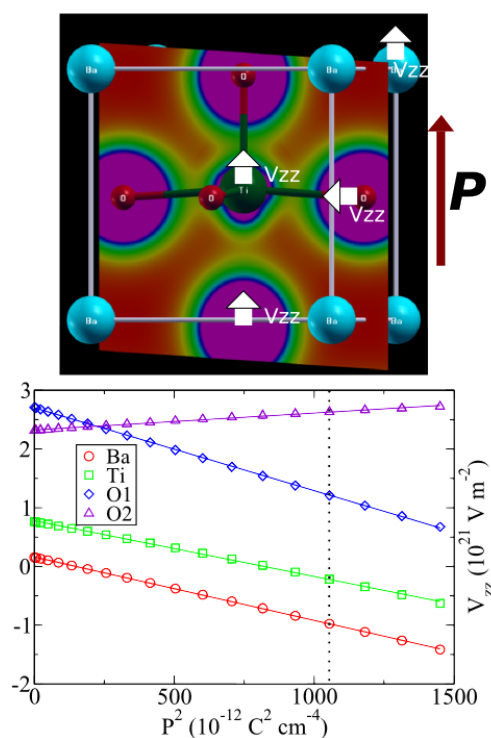


**Fig. 1:** Top) picture of the experimental structure of BaTiO<sub>3</sub> showing the direction of V<sub>zz</sub> (main component of the EFG) at some atoms and the polarization. Bottom) V<sub>zz</sub> (largest EFG component) as a function of the polarization squared, showing a linear relationship. The dotted line corresponds to the values calculated with the experimental tetragonal structure at equilibrium conditions.

*J.N. Gonçalves (for the IS487 Collaboration)*

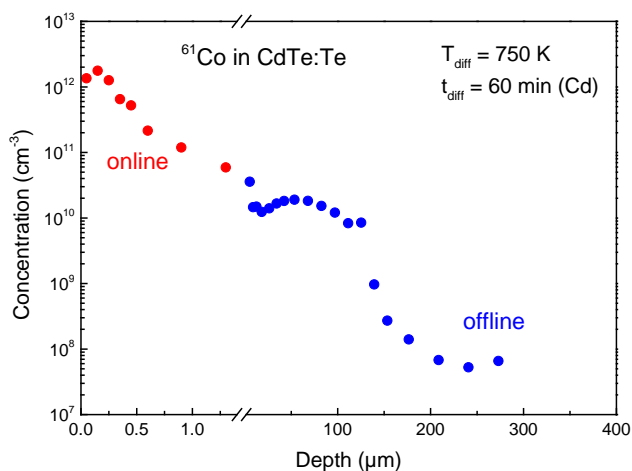
## IS489: First results with the online diffusion setup at ISOLDE

An active programme exploring radiotracer diffusion in semiconductors has been underway at ISOLDE for many years and in recent times has focused on the anomalous diffusion profiles of dopants in compound semiconductors such as CdTe [2,3]. Up to now, the diffusion profile has been determined after implantation and diffusion annealing using offline sectioning of the samples by mechanical polishing. This technique limits the range of usable radioactive isotopes to half-lives longer than about 1 hour and the achieved diffusion lengths have to be in the order of several 10 μm. This has meant that some highly interesting cases such as magnetic dopants in semiconductors and long-standing questions such as self-diffusion in Al have been excluded from the experimental programme.

In the summer of 2011, an online diffusion chamber which allows us to close this gap was delivered to ISOLDE, installed and tested [3]. This chamber incorporates all the elements required for radio-tracer measurements, but every step is carried out in situ, without breaking the vacuum.

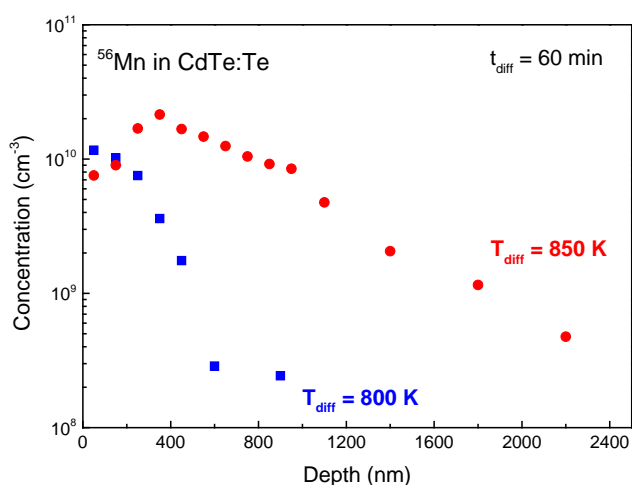
In November/December 2012, the online diffusion chamber was used for the first measurements of the diffusion of magnetic impurities in CdTe.

Fig. 1 shows the results obtained for the diffusion of <sup>61</sup>Co in Te-rich CdTe annealed after implantation at 750 K under external Cd pressure for 60 min. The diffusion profile up to a depth of 1 μm has been obtained using the online setup and sectioning by Ar sputtering, the profile from 1 μm to 300 μm was obtained by offline mechanical polishing. For the first time we now have a complete picture for the unusual diffusion behaviour of Co in CdTe throughout the crystal from front to back.



**Fig. 1:** Diffusion profile for  $^{61}\text{Co}$  in Te-rich CdTe obtained after annealing under external Cd pressure and measured using the online diffusion chamber (red points) and sectioning by mechanical polishing (blue points).

The diffusion of  $^{56}\text{Mn}$  in Te-rich CdTe annealed at 800 K and 850 K, respectively, in vacuum after implantation is shown in Fig. 2. The shallow diffusion profile was measured using the online diffusion chamber. Earlier measurements [4] using sample sectioning by chemical etching required higher annealing temperatures and annealing times up to weeks.



**Fig. 2:** Diffusion profile of  $^{56}\text{Mn}$  implanted into Te-rich CdTe. The profiles have been obtained after annealing in vacuum at 800 K and 850 K using the online diffusion chamber.

[1] H. Wolf, F. Wagner, Th. Wichert, and ISOLDE Collaboration, Phys. Rev. Lett. 94, 25901 (2005).

[2] H. Wolf, J. Kronenberg, F. Wagner, Th. Wichert, and ISOLDE Collaboration, Phys. Status Solidi B 247, 1405 (2010).

[3] ISOLDE newsletter Spring 2012, p. 18.

[4] N.Y. Jamil and D. Shaw, Semicond. Sci. Technol. 10, 952 (1995).

*M. Deicher*

## IS496: First measurement of the $B(E2; 2^+_1 \rightarrow 0^+_1)$ value of $^{142}\text{Sm}$

The second part of IS496, aiming at Coulomb excitation of neutron-deficient, radioactive  $^{142}\text{Sm}$ , was conducted from June 28<sup>th</sup> to July 1<sup>st</sup> 2012, subsequent to last year's measurement on  $^{140}\text{Nd}$ . Both experiments will help to investigate the evolution of the E2 transition strengths of the first excited  $2^+$  states in the N=80 isotonic chain. This allows the study of the effect of shell stabilization of the collective isovector valence-shell excitations [1, 2]. In order to be able to interpret the data around the Z=56 subshell closure the missing transition strength of  $^{142}\text{Sm}$  is necessary. It is also required in preparation of future HIE-ISOLDE experiments for both isotopes (proposal accepted), where higher-lying mixed-symmetry states will be investigated.

A newly developed RILIS ionization scheme for  $^{142}\text{Sm}$  was used and the fraction of isobaric contamination was determined in a combination of laser-on/-off runs and short thick target runs, where the decay lines could be observed. Coulomb excitation data was taken for about 34 hours. The beam ions were impinging on a  $1.4 \text{ mg/cm}^2$   $^{48}\text{Ti}$  as well as on a  $2 \text{ mg/cm}^2$   $^{94}\text{Mo}$  target with 2.85 MeV/u. Fig. 1 shows the random-background subtracted gamma-ray spectra, Doppler-corrected for A=142 beam particles as well as for target recoils. These spectra

show only the transitions from the first excited  $2^+$  states to the  $0^+$  ground state in  $^{142}\text{Sm}$ ,  $^{48}\text{Ti}$  and  $^{94}\text{Mo}$ , respectively. Using normalization on the well-known target excitation cross-sections, the Coulomb-excitation cross-section of  $^{142}\text{Sm}$  could be determined. A successive analysis by variation of the transitional and diagonal matrix elements with the computer codes CLX and DCY [3] determined the  $B(E2; 2^+_1 \rightarrow 0^+_{gs})$  value of  $^{142}\text{Sm}$  preliminary to be **29(2) W.u.**

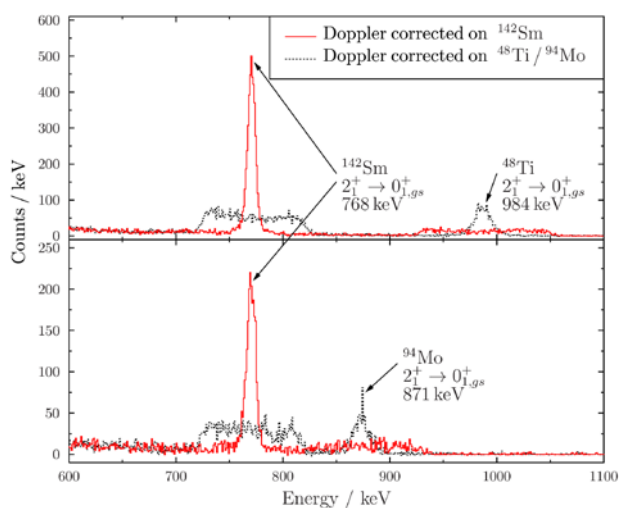


**Fig.1:** Doppler corrected  $\gamma$ -ray spectra after subtraction of random background. The Doppler correction was done either with respect to the projectile or the target

This result deviates from recent QPM calculations for  $N=80$  isotones, which yield 22 W.u. [4], while it is in agreement with state-of-the-art large-scale shell model calculations, yielding 27.4 W.u. [5]. This finding provides a benchmark for the foreseen investigation of the effect of shell stabilization of the quadrupole isovector valence-shell excitations.

[1] N. Pietralla et al., INTC P-268 (2009)

[2] G. Rainovski et al., PRL 96, 122501 (2006)

[3] H. Ower, PhD thesis

[4] N. Lo Iudice et al., PRC 77, 044310 (2008)

[5] D. Bianco et al., PRC 85, 034332 (2012)

*R. Stegmann and C. Bauer*  
(for the IS496 collaboration)

## IS497: Collinear Laser Spectroscopy of cadmium: probing the nuclear structure in the region of the neutron 50 and 82 shell closure

The cadmium chain has been investigated from  $N=52$  to the  $N=82$  shell closure by the COLLAPS collaboration using collinear laser spectroscopy. Besides the ground states, the long-lived  $I=11/2^-$  isomers were studied. Thereby, the  $^{127m,129m}\text{Cd}$  isomers were observed for the first time.

The measurements have been carried out in three runs. In August 2011 we started with the spectroscopy of the isotopes closer to stability. We probed the atom using a transition from the metastable  $5s5p\ ^3P_2$  state to the  $5s6s\ ^3S_1$  state at a wavelength of 509 nm.

The two runs in April 2012 aimed at more exotic isotopes and were performed on the cadmium ions due to a higher sensitivity. Here, the transition from the  $5s\ ^2S_{1/2}$  ground state to the  $5p\ ^2P_{3/2}$  excited state at a wavelength of 214.5 nm was used. This is to our knowledge the deepest UV transition which was used for collinear laser spectroscopy so far.

The required wavelength was produced by frequency quadrupling of 860-nm light provided by a continuous-wave Ti:Sa laser. Two steps of cavity-enhanced second-harmonic generation in a nonlinear crystal were employed. About 20 mW of laser power in the UV was obtained with measured power fluctuations below three percent.

Figure 1 shows the hyperfine structure of the  $I=3/2^+$  state and the  $I=11/2^-$  state of

the  $^{129}\text{Cd}$  ion as an example. Both states are clearly distinguishable from each other. However, a decision on which spin-state is the ground-state and which one the isomer, is not possible based on our data.

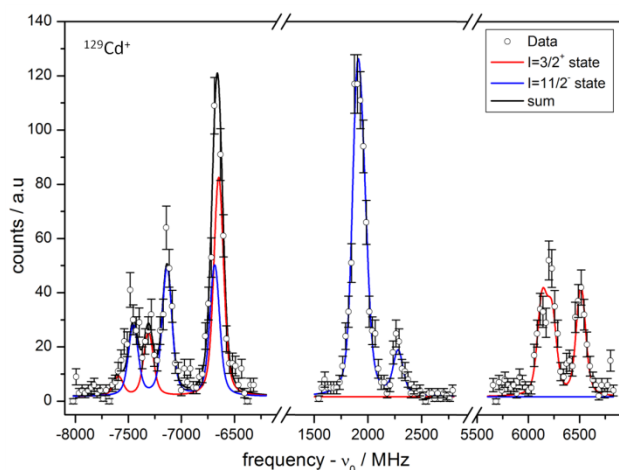


**Fig.1:** Hyperfine structure of the  $I=3/2^+$  state (red) and the  $I=11/2^-$  state (blue) of  $^{129}\text{Cd}^+$ . The black curve is the fit result for the combined hyperfine structure.

Several nuclear properties of the ground state and the isomeric state can be determined from the measured hyperfine structure: the nuclear spin, the nuclear magnetic moment, the electric quadrupole moment and the charge radius. Data analysis is still ongoing.

The nuclear spin of  $^{119}\text{Cd}$  could be unambiguously determined from the number of resonances in the hyperfine structure to be  $I=1/2$ . This contradicts the previously reported value of  $I=3/2$  [1].

The studied electric quadrupole moments of the  $I=11/2^-$  state of  $^{111}\text{Cd}$  to  $^{129}\text{Cd}$  increase linearly as a function of the neutron number. This is predicted in the spherical shell model. Surprisingly, this behaviour continues beyond the expected extent of maximum occupancy of the  $h_{11/2}$  neutron shell [2].

[1] D. M. Szymochko et al., Nucl. Data Sheets 110, 2945 (2009)

[2] D. T. Yordanov et al., accepted for publication in PRL(2013)

*Nadja Frömmgen and Michael Hammen for the COLLAPS Collaboration*

## IS505: Study of the deuteron emission in the $\beta$ decay of $^6\text{He}$

The  $\beta$  decay of  $^6\text{He}$  ( $T_{1/2}=807$  ms) offers a sensitive probe to study its relatively simple two-neutron halo structure ( $\alpha+2n$ ). With a very small branching ratio ( $\approx 10^{-6}$ ) this decay proceeds to the final state of an  $\alpha$  particle and a deuteron [1]. The probability of this  $\beta$ -delayed deuteron ( $\beta d$ ) emission, and the spectrum of deuterons, is very sensitive to details of the initial  $^6\text{He}$  wave function. The continuous  $\beta d$  spectrum has been determined, however, only for the decay energies larger than 400 keV in the  $\alpha+d$  center of mass [2,3]. The reason for this threshold was pile-up and summing effects induced in silicon detectors by electrons emitted in the dominant decay channel of  $^6\text{He}$ .

The shape and the intensity of the low-energy part of the  $\beta d$  spectrum would help to constrain model parameters, and thus lead to better understanding of the structure of the initial halo wave function of  $^6\text{He}$ . To meet this challenge we applied a different detection technique employing the Optical Time Projection Chamber (OTPC) [4]. The OTPC records tracks of charged particles, like ions,  $\alpha$ -particles or deuterons, while remaining insensitive to  $\beta$ -rays. The full 3D reconstruction of the tracks combines the 2D image of the decay taken by a CCD camera and the drift-time profile measured by a photomultiplier. The experiment was performed in August 2012. The ions of  $^6\text{He}$ , produced in a  $\text{UC}_x$  target and selected with the GPS separator, were subsequently bunched and accelerated to 3 MeV/u by REX-ISOLDE and finally implanted

into the active volume of the OTPC filled with a gas mixture of 98% He + 2% N<sub>2</sub> at the atmospheric pressure. After implantation of each bunch, containing about 10<sup>4</sup> ions of <sup>6</sup>He, the CCD exposure and the drift-time profile recording were started for a period of 800 ms. Decay events of <sup>6</sup>He into an α particle and a deuteron were clearly observed – an example is shown in Fig. 1. Preliminary analysis indicates that events corresponding to the center-of-mass decay energy of down to 150 keV can be safely reconstructed, which illustrates the advantage of this technique. In addition, about 30% of events are found in the low-energy part of the spectrum, below 400 keV, which could not be accessed in previous experiments. We may anticipate that the full analysis of the collected data will shed new light on the two-neutron halo of <sup>6</sup>He.

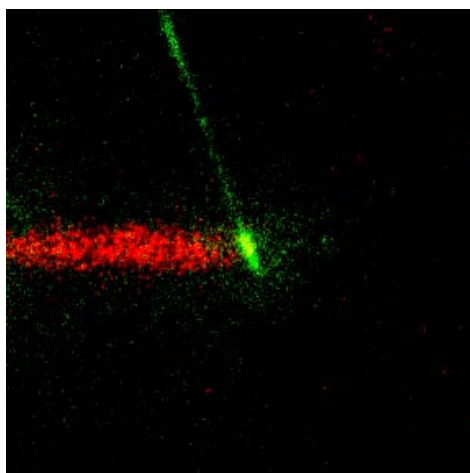


**Fig.1:** The overlap of two photographs, taken by a CCD camera, shows a bunch of <sup>6</sup>He ions implanted into the OTPC (red) and a decay event of <sup>6</sup>He in which the final nucleus breaks into a deuteron and an alpha particle flying in opposite directions (green).

[1] K. Riisager et al., Phys. Lett. B 235, 30 (1990).

[2] D. Anthony et al., Phys. Rev. C 65, 034310 (2002).

[3] R. Raabe et al, Phys. Rev. C 80, 054307 (2009).

[4] K. Miernik et al., Nucl. Instr. and Methods A 581, 194 (2007).

*Marek Pfützner*

## IS507: Study of the beta-decay of <sup>20-21</sup>Mg

The beta-decay of the dripline nucleus <sup>20</sup>Mg gives important information on resonances in <sup>20</sup>Na, which are relevant for the astrophysical rp-process. In particular the spin and parity of the 2645 keV level in <sup>20</sup>Na is unsettled. This resonance is situated in the Gamow-window of the <sup>19</sup>Ne(p,γ)<sup>20</sup>Na reaction from the breakout sequence of the HCNO cycle and is thus essential to understand the reaction rate.

In order to settle this question the IS507 experiment was the first to study the beta-decay of <sup>20</sup>Mg at an ISOL facility. Earlier experiments have been performed at RIKEN [1], MSU [2], GANIL [3], and Texas A&M [4] – all in-flight facilities. The ability of producing <sup>20</sup>Mg at ISOLDE gives some new possibilities in terms of studying the decay products. First of all the better separation of the nuclei at ISOL facilities compared to in-flight gives a less contaminated ion beam. In this sense we obtain a much cleaner spectrum of the decay. Secondly, the lower energy of the ion beam allows for implantation in a thin window of e.g. a Gas-Si telescope.

The advantage of using a Gas-Si telescope is the possibility of making ΔE-E plots. This allows for a direct distinction of the various decay branches, which is demonstrated in figure 1. Data from the beta decay of <sup>21</sup>Mg is shown, which were used for calibration purposes. One clearly sees a so far unknown decay branch with beta-delayed alpha particle emission. Further analysis is needed to characterize this decay mode.

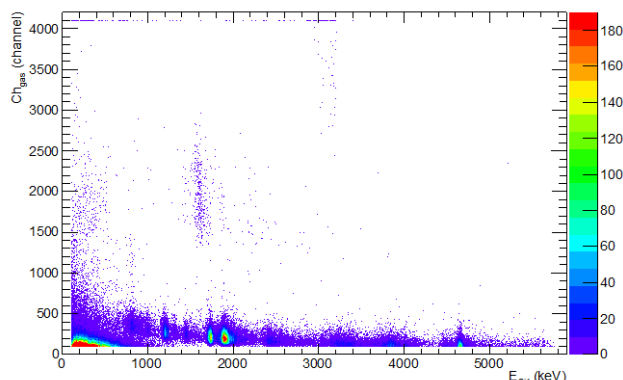


**Fig. 1:**  $\Delta E$ - $E$  plot using the Gas-Si telescope of the beta decay of  $^{21}\text{Mg}$ .

The energy spectrum of  $^{20}\text{Mg}$  from a Si detector in the Gas-Si telescope is shown in figure 2. The analysis is not yet completed. For the production of Mg a SiC target with the W ion source and RILIS were used. For separation of  $^{20}\text{Mg}$  from the main contaminant,  $^{20}\text{Na}$ , the HRS with the slits in was used. This resulted in an observed yield of 34  $^{20}\text{Mg}/\mu\text{C}$  and 860  $^{21}\text{Mg}/\mu\text{C}$  assuming a 10% transmission to the setup.

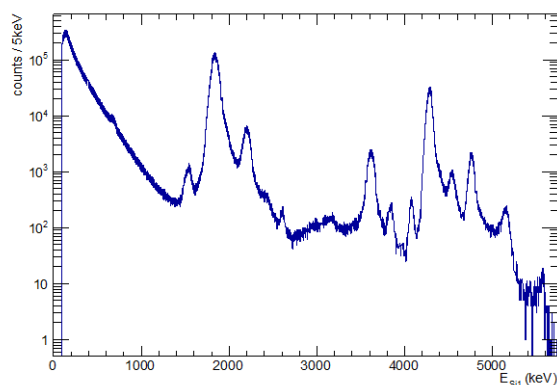


**Fig. 2:** Energy spectrum of the beta-delayed particles from  $^{20}\text{Mg}$ .

- [1] S. Kubono *et al.*, Phys. Rev. C46 (1992) 361.
- [2] J. Görres *et al.*, Phys. Rev. C46 (1992) R833.
- [3] A. Piechaczek *et al.*, Nucl. Phys. A 584 (1995) 509.
- [4] J.P. Wallace *et al.*, Physics Letters B 712 (2012) 59-62.

*Morten V. Lund (for the MAGISOL Collaboration)*

## IS508: Spin, moment and charge radii measurements of manganese isotopes

High resolution laser spectroscopy of neutron-rich manganese isotopes was performed in November 2012. Full hyperfine structures of the  $^{51,53-64}\text{Mn}$  ground states were measured, in addition to those of the isomeric states in  $^{58,60,62}\text{Mn}$ . This has enabled the nuclear spin, magnetic dipole moment, electric quadrupole moment and the change in mean-square charge radius to be determined for all of these states.

In the collinear laser spectroscopic method, the laser and ion/atom beams are overlapped in a parallel geometry and fluorescence photons detected using a quartet of photomultiplier tubes for high detection efficiency. Ions were accumulated and released in bunches from ISCOOL in order that the photon background caused (at a continuous rate) by the scattering of laser light could be suppressed by four orders-of-magnitude. An additional gate was applied to the proton trigger to enhance the signal-to-noise ratio of the shorter-lived states and, in some cases, to discriminate against longer-lived (isomeric) states. An example spectrum is shown in Figure 1.

Prior to this work, a dearth of known ground state properties in the region was evident. In particular, few spin assignments had been reliably made. These results not only determine unambiguously the nuclear spins of the ground and isomeric states, but will be crucial in making assignments for the shorter-lived excited states.

Meanwhile, shell model calculations with various interactions will be compared. The new experimental data will provide a stringent assessment of their various predictions, while a comparison of the magnetic moments in particular offers a

sensitive probe of the nuclear wave function. Furthermore, subshell effects at  $N=32,34$ , if present, will reveal themselves as minima in the course of the charge radii.

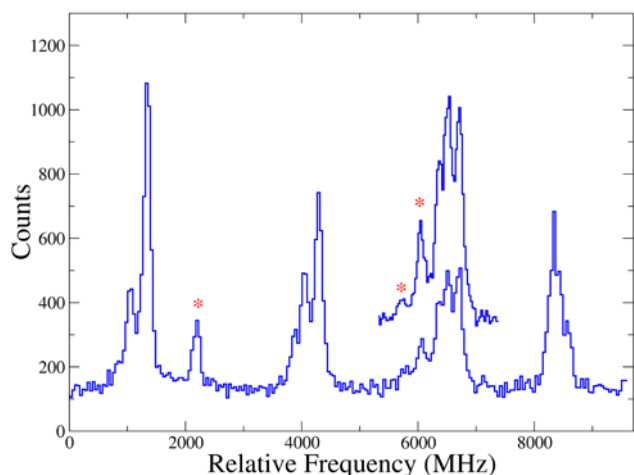


**Fig.1:** Full hyperfine structure of the  $^{60}\text{Mn}$  ground state and isomer. For illustration, asterisks indicate only those peaks of the low-spin state which are fully resolved by eye.

These measurements were undertaken by exciting a transition from the atomic ground state and take us tantalisingly close to  $N=40$  ( $^{65}\text{Mn}$ ) in a region where an onset of deformation has been predicted and a new “island of inversion” is thought to occur. Following the realignment of ISCOOL (currently underway) in-cooler optical pumping will be established [1]. This will enable population enhancement of a single electronic energy level of the ion and the study of a transition from this state. With the expected increase in spectroscopic efficiency, isotopes beyond  $N=40$  will then be explored.

[1] F.C. Charlwood et al. Phys. Lett. B 690 (2010) 346–351

*B. Cheal (for the COLLAPS Collaboration)*

## IS518 and IS534: Charge radii and masses of gold and astatine isotopes

During the 2012 experimental campaign, the experiments IS518 and IS534 aimed at complementary studies of shape coexistence and ground state properties in the long series of gold ( $^{177-182,185,191}\text{Au}$ ) and astatine ( $^{197,198,203,205,207,209,211,217}\text{At}$ ) isotopes. A broad range of phenomena, e.g. the onset of quadrupole, octupole and triaxial deformation, including shape staggering, is expected to occur in some of these nuclides. Signatures of these phenomena can be observed through macroscopic nuclear properties, such as binding energies and charge radii.

Two types of measurements were conducted: hyperfine-structure (HFS) and charge-radii studies by in-source laser spectroscopy with the RILIS laser system and Penning-trap mass spectrometry of nuclear ground and isomeric states.

In the IS534 experiment, the laser-ionized and mass-separated 50-keV ions were implanted in a carbon foil of the Windmill (WM) system [1]. The alpha and gamma decays of the implanted activity were detected with a set of silicon and germanium detectors surrounding the implantation foil. By counting the number of alpha or gamma decays of a specific isotope as a function of laser wavelength, its HFS was recorded.

The ISOLTRAP experiment accumulates, cools and bunches the quasi-continuous beam from ISOLDE by using a buffer-gas filled, segmented, linear radiofrequency quadrupole (RFQ) [2]. Placed after the RFQ, a multi-reflection time-of-flight mass separator (MR-TOF MS) [3] ensures a separation of different isobars from ISOLDE, as shown in Fig. 1 for the case of the  $A = 207$  beam. During the present

campaign, the MR-TOF MS was used in two different modes.

For Penning-trap mass measurements, the TOF-separated beam was purified by a Bradbury-Nielsen ion gate, with a mass resolving power of the order of  $10^5$  achieved for only 30 ms trapping time. Thus, only the ions of interest entered the Penning trap for the actual precision mass measurement, using the time-of-flight ion-cyclotron-resonance technique [4].

For the in-source laser spectroscopy measurements, the TOF spectrum was measured on an electron multiplier placed after the MR-TOF MS. By monitoring the ions of interest, e.g. the  $^{207}\text{At}$  peak in Fig. 1, and varying the wavelength of the RILIS lasers, it was possible to perform the in-source laser spectroscopy with MR-TOF beam analysis resulting in little to no background from contaminating isobars.

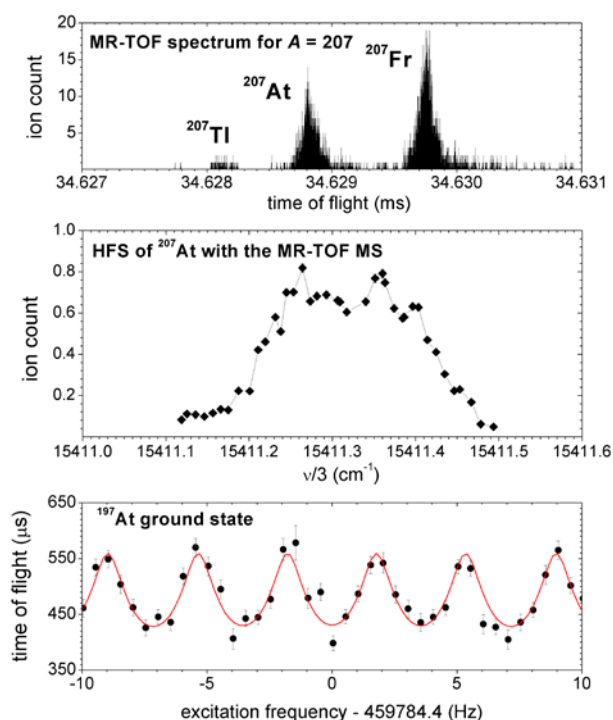


**Fig. 1:** MR-TOF spectrum for mass  $A = 207$  (upper panel); HFS in narrow-band laser mode of  $^{207}\text{At}$  (middle panel) obtained by monitoring the  $^{207}\text{At}$  peak in the upper panel; Ramsey-type Penning-trap measurement of the  $^{197}\text{At}$  ground state (lower panel).

Using either the WM or the MR-TOF MS detection methods for the in-source laser spectroscopy (depending on the half-life and the production rate of the isotope of interest), the HFS of  $^{177-182,185,191}\text{Au}$  and  $^{197,198,203,205,207,209,211,217}\text{At}$  were measured.

Some spectra were recorded in a narrow-band laser mode, others only in a broad-band mode, the latter yielding a lower-resolution HFS spectrum. In the case of isotopes with isomeric states, the alpha-energy selectivity of the Windmill experiment (IS534) allowed to separately investigate the HFS of the isomeric and ground states. This information was then used to selectively ionize the isomeric or ground state or to adjust their ratio in the ISOLDE beam, by tuning the wavelength of the RILIS scanning step. Taking the selectively-ionized beams to the Penning trap, the excitation energy of the isomeric states was determined, as in the case of  $^{197}\text{At}$ , for which a Ramsey-type Penning-trap measurement is shown in Fig. 1. A new alpha-decaying isomer was found in  $^{178}\text{Au}$ , whose HFS is completely different from the one of the second  $^{178}\text{Au}$  alpha-decaying state. They are denoted as m1 and m2 in Fig. 2. In the future, experiments with pure isomeric beams of  $^{178}\text{Au}$  are possible.

Before our measurements, the charge radii in the gold isotopic chain were known for  $^{183-200}\text{Au}$  [5]. A gradual increase of the deviation from radii deduced from a spherical liquid drop model was observed by approaching  $^{187}\text{Au}$  followed by a sudden onset of deformation observed in  $^{186}\text{Au}$ . The  $^{183-186}\text{Au}$  isotopes possess a deformation of  $\beta_2 \sim 0.27$ , typical for prolate-deformed nuclei in this region. Predictions for the charge radii suggest a sudden jump back to sphericity for the lighter Au isotopes [6]. Our new HFS measurements in the gold isotopic chain extend the previously known data up to  $^{177}\text{Au}$  ( $N = 98$ ). The data analysis is underway.

The astatine measurements result from an exploratory program for developing astatine beams at ISOLDE (LOI86) for laser spectroscopy, beta-delayed fission (IS534) and mass measurements (IS518). The measurements became possible due to the recent development of the laser-ionized astatine beam at ISOLDE [7].

The synergy between the RILIS, WM and MR-TOF MS has thus proven to be extremely beneficial both for the HFS studies and for the Penning-trap mass spectrometry.

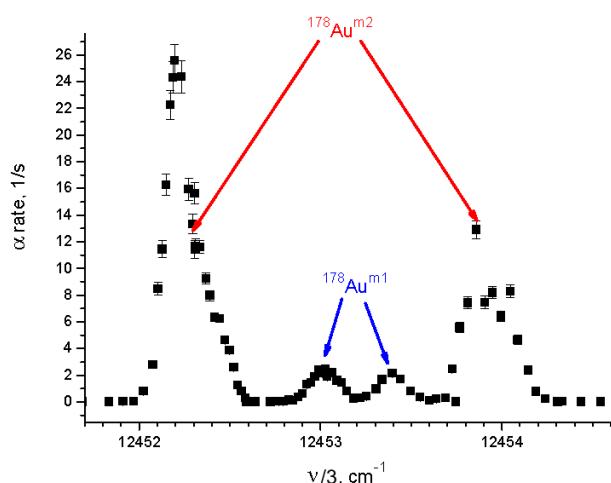


**Fig.2:** HFS in broadband laser mode for  $^{178}\text{Au}$ , measured with the WM experiment

- [1] A. Andreyev *et al.*, Phys. Rev. Lett. 105, 252502 (2010).
- [2] F. Herfurth *et al.*, Nucl. Instrum. Meth. A 469, 254 (2001).
- [3] R. Wolf *et al.*, Nucl. Instr. and Meth. A 686, 82 (2012).
- [4] M. König *et al.*, Int. J. Mass Spectrom. Ion. Process. 142, 95 (1995).
- [5] K. Wallmeroth *et al.*, Phys. Rev. Lett. 58, 1516 (1987); U. Krönert *et al.*, Z. Phys. A 331, 521 (1988).
- [6] J.L. Wood *et al.*, Nucl. Phys. A 651, 323 (1999).
- [7] S. Rothe *et al.*, Nat. Commun., accepted.

*A. Andreyev (for the Astatine and Windmill Collaborations) and V. Manea (for the ISOLTRAP Collaboration)*

## IS520: Study of $^{13}\text{Be}$ through isobaric analog resonances in the Maya active target

Experiment IS520 aimed at studying the low-lying states in the unbound system  $^{13}\text{Be}$ . The determination of their sequence can shed light on the evolution of the  $N = 8$  shell closure towards the dripline.  $^{13}\text{Be}$  also provides important information for the modelling of the two-neutron halo nucleus  $^{14}\text{Be}$ .

For this study we populated the isobaric analog resonance in  $^{13}\text{B}$  through the resonant scattering of  $^{12}\text{Be}$  nuclei on protons. Once the IAS is populated, isospin conservation allows decay via emission of a proton that will be detected in our setup.

The  $^{12}\text{Be}$  beam (post-accelerated for the first time in REX) was sent into Maya [1], an active target, in which the detection gas, isobutane, contained the protons that were the target of the reaction.

Maya is a gaseous detector, allowing a three-dimensional reconstruction of the tracks of the charged particles traversing the gas volume. If an incident beam particle undergoes a nuclear reaction with one of the gas atoms, the exact position of the reaction vertex and the energies and angles between the outgoing reaction products can be deduced.

An array of Si and CsI detectors covers the wall opposite the beam entrance, to detect forward-emitted light ions which are not stopped in the gas volume.

An important problem was represented by the contamination of  $^{12}\text{C}^{4+}$  ions in the  $^{12}\text{Be}$  beam. Indeed,  $^{12}\text{C}$  was about  $10^4$  times more intense than  $^{12}\text{Be}$  in our detector.

A performance check of the setup and the analysis method can be done by investigating known resonances in  $^{13}\text{N}$ . The resulting proton spectrum clearly shows the two closely-lying resonances in  $^{13}\text{N}$  ( $E^* =$

3.50 and 3.55 MeV, corresponding to  $E_p \sim 4.9$  MeV), as can be seen in Fig.1.

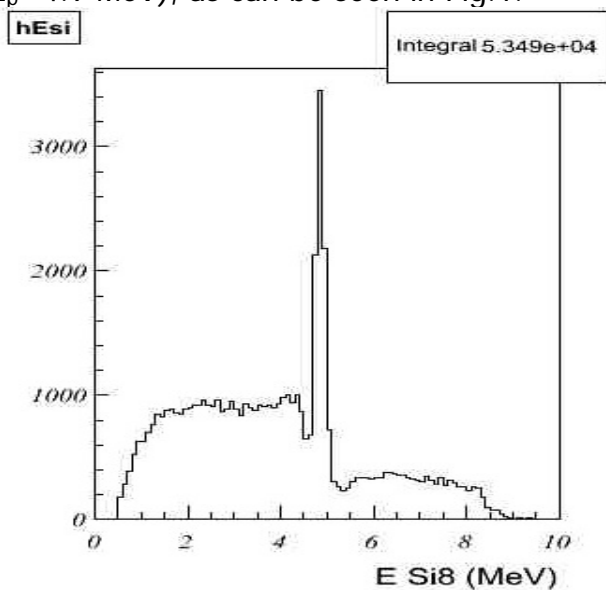


**Fig.1:** Experimental spectrum of protons from the scattering of  $^{12}\text{C}$ . The energy is the one measured by the silicon placed downstream.

Identification of the particles is achieved via the specific energy loss, the total energy deposited and the length of the paths. In Fig.2, the energy loss of non-interacting  $^{12}\text{Be}$  beam ions during their travel through Maya is shown.

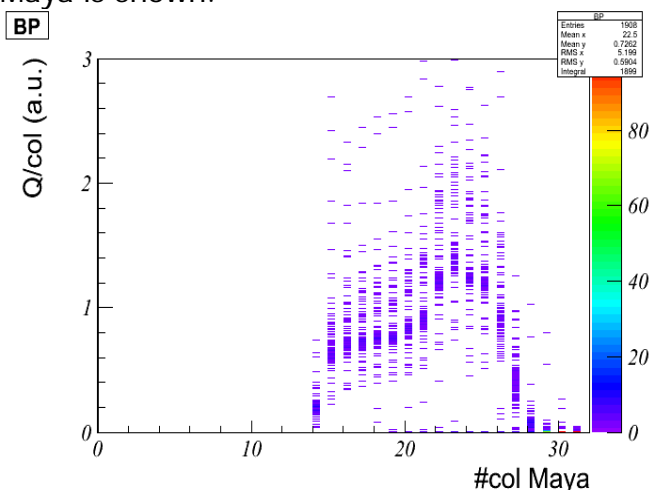


**Fig.2:** Bragg curve of non-interacting  $^{12}\text{Be}$  beam ions. The first part of Maya was masked to avoid the intense signals from  $^{12}\text{C}$ .

[1] Demonchy et al, NIMA 583 (2007) 341–349

Sara Sambi for the IS520 Collaboration

## IS524: Coulomb excitation of $^{123}\text{Cd}$

Below the  $Z=50$  proton shell closure, the Cadmium isotopic chain with 48 protons remains highly interesting for the nuclear structure physics. The neutron-rich even-even Cadmium isotopes have been successfully studied with  $\gamma$ -ray spectroscopy following “safe” Coulomb excitation (IS411, IS477). Surprisingly they show signs of collectivity larger than predicted by modern shell-model calculations [1, 2]. Aiming for a better understanding of how collectivity may arise in the hole-hole nuclei it is essential to study the odd-A nuclei here, where the roles played by different orbits can be determined. In a first campaign, the isotope  $^{123}\text{Cd}$  has been investigated because its level scheme was believed to be well known.

Recently, mass measurements with the double Penning trap JYFLTRAP were carried out in order to investigate isomeric states in nuclei near the doubly magic nucleus  $^{132}\text{Sn}$ . For the  $11/2^-$  isomeric state of  $^{123}\text{Cd}$  the time-of-flight ion cyclotron resonance technique yielded an energy of 144(4) keV [3] which is in conflict with the energy of 316.53 keV determined in a previous study [4]. Obviously, a revision of the level scheme is necessary.

In parallel, the Cadmium isotopes have also been investigated by COLLAPS (IS497). Their results for the long-living ground state and  $11/2^-$  isomer obtained with laser spectroscopy will complement the results of the Coulomb excitation experiment leading to a comprehensive picture of  $^{123}\text{Cd}$ .

The exotic isotope  $^{123}\text{Cd}$  was produced at ISOLDE using the RILIS ion source to provide clean Cadmium beams and post-accelerated by REX. A beam of  $^{123}\text{Cd}$  composed of both the ground and the isomeric state with an energy of 2.85 MeV/A was delivered to the MINIBALL set-up. For

Coulomb excitation of the beam particles a  $^{64}\text{Zn}$  target with a thickness of  $1.55\text{ mg/cm}^2$  was used. Both the scattered projectile and recoiling target nuclei were detected with a double-sided silicon strip detector (DSSSD). The MINIBALL spectrometer was used for detecting  $\gamma$ -rays from the de-excitation of the  $^{123}\text{Cd}$  and  $^{64}\text{Zn}$  nuclei in coincidence with events of the DSSSD.

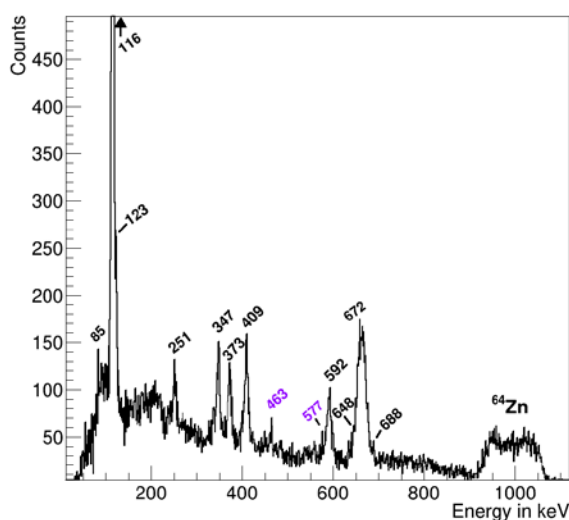


**Fig.1:** Projectile Doppler corrected  $\gamma$ -spectrum: besides the already known  $\gamma$ -energies *new transitions* have been found

The set-up allows for Doppler correction of the  $\gamma$ -rays with respect to the particles detected on the DSSSD. In the Doppler corrected  $\gamma$ -ray spectrum, shown in Fig. 1, several transitions originating from  $^{123}\text{Cd}$  are observed. From these data, a level scheme can be constructed using  $\gamma\gamma$ -coincidences.

After establishing the level scheme, a determination of the  $B(E2)$  values will be possible offering a deeper insight into the evolution of collectivity along the Cadmium isotopic chain.

[1] S. Ilieva et al., in preparation

[2] Th. Behrens, PhD Thesis, Technische Universität München, 2009

[3] A.Kankainen et al., arXiv:1206.6236v1

[4] H. Huck et al., Phys. Rev. C 40, 1384 (1989)

A.-L. Hartig, S. Ilieva

## IS532: Precision mass measurements of neutron-rich calcium isotopes

During the running campaign of 2012, the ISOLTRAP experiment [1] successfully determined the masses of  $^{53,54}\text{Ca}$ , which have eluded measurements so far. These measurements were made possible by a breakthrough in mass-spectrometry techniques. The results were obtained using the recently installed multi-reflection time-of-flight mass separator (MR-TOF MS) [2] as a spectrometer, together with an ion detector.

The MR-TOF MS resolves the isobars in the time-of-flight spectrum on the detector, which can be turned into a mass spectrum by calibrating the device with reference ions of known mass. To this end, the isobars in the ISOLDE beam that are usually considered as contaminants are turned into an obvious advantage, serving as reference masses complementing the alkali ions from the ISOLTRAP off-line ion source.

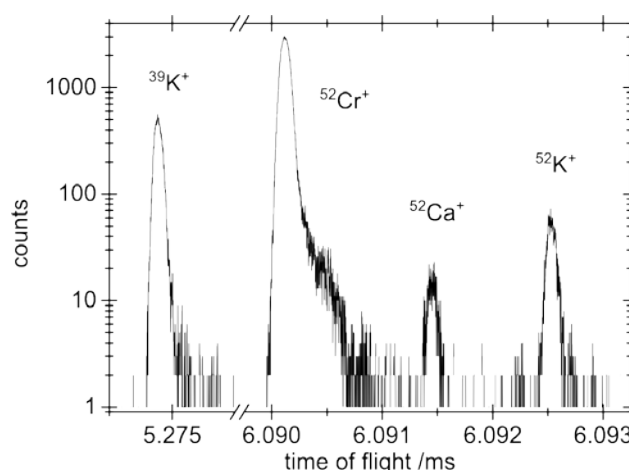


**Fig.1:** Time-of-flight spectrum of singly-charged  $A=52$  isobars and the reference ion  $^{39}\text{K}^+$  from the off-line source (for details see text).

Prior to the calcium mass measurements, the MR-TOF mass-spectrometric method was commissioned both off- and on-line with several nuclides of well-known mass.

Figure 1 shows an example of the time-of-flight spectrum for mass number  $A = 52$  from the calcium run, where the masses of  $^{52}\text{Ca}$  and  $^{52}\text{K}$  were determined using as reference ions  $^{39}\text{K}^+$  and  $^{52}\text{Cr}^+$ . The result for  $^{52}\text{Ca}$  was compared to a conventional Penning-trap measurement through the time-of-flight ion-cyclotron-resonance (TOF-ICR) technique [3], performed not only at our setup but also at TRIUMF by the TITAN Penning-trap experiment [4]. The relative uncertainty obtained through the mass measurement using the MR-TOF MS is comparable to that quoted in [4], and the result agrees well with the TOF-ICR result. With a much shorter measurement time than the one typically required for a Penning-trap measurement, the MR-TOF MS is expected to become an indispensable instrument for the measurement of low-yield, short-lived isotopes.

The experimental masses have an immediate impact on the theoretical description of nuclear structure far from stability [5]. They serve as anchor points for structural effects at  $N = 32$  as well as for reliable predictions of masses towards the neutron drip line. Moreover, the new masses provide a stringent test of microscopic calculations with three-nucleon forces derived from state-of-the-art chiral effective-field theory.

- [1] M. Mukherjee *et al.*, Eur. Phys. J. A 35, 31 (2008)
- [2] R. N. Wolf *et al.*, Nucl. Instr. and Meth. A 686, 82 (2012)
- [3] M. König *et al.*, Int. J. Mass Spectrom. Ion. Process. 142, 95116 (1995)
- [4] A. T. Gallant *et al.*, Phys. Rev. Lett. 109, 032506 (2012)
- [5] F. Wienholtz *et al.*, submitted (2013)

*S. Kreim (for the ISOLTRAP Collaboration)*

## IS536: Gamma spectroscopy and shape transitions in $A \approx 100$ neutron-rich nuclei populated by $^7\text{Li}$ cluster transfer reactions.

Neutron-rich nuclei with  $A \approx 100$  are of particular interest for the study of nuclear structure and shell evolution toward the neutron drip-line. The region around  $N=60$  is characterized by shape transition from a partial sub-shell closure at  $N=56$  to a stable deformation at  $N=60$ . Such behaviour is confirmed by experimental studies of the  $2_1^+$  energies as well as the  $4_1^+/2_1^+$  energy ratios, which clearly show an onset of stable deformation at  $N=60$  in different isotopic chains [1-2]. Furthermore, several rotational bands have been observed in nuclei with  $N \geq 60$ , as a confirmation of the well-deformed structure in this mass region [3]. The available experimental data are usually limited to yrast states while information on non-yrast states is needed to further study this phenomenon. The combination of radioactive beams and cluster transfer reactions may represent a powerful tool to investigate neutron-rich nuclei at moderately high spin and energy. The weakly bound  $^7\text{Li}$  is particularly suitable for this purpose: owing to a separation energy of  $\approx 2.5$  MeV,  $^7\text{Li}$  easily breaks up into  $\alpha$  and  $t$  clusters, which have a significant probability of being captured. Such a process has a high and positive  $Q$ -value, so that the transfer usually takes place at high excitation energy favouring the population of medium-high spin states, as observed in direct kinematics  $^7\text{Li}$ -induced reactions [4]. The experiment presented in this work aims at studying  $n$ -rich  $^{98,99,100}\text{Sr}$  isotopes. It has been performed in November 2012 at ISOLDE, using the MINIBALL-T-REX setup [5]. A  $^{98}\text{Rb}$  beam, with average intensity of  $10^5$  pps, was accelerated to 2.85 MeV/A and directed onto a  $1.5 \text{ mg/cm}^2$  thick  $^7\text{LiF}$

target. Sr isotopes arising from t-transfer to  $^{98}\text{Rb}$  are uniquely associated with  $\alpha$  emission, whose detection in the CD detector produced a clean trigger for the  $^7\text{Li}(^{98}\text{Rb}, \alpha X \gamma)$  process. A very preliminary analysis shows that the emitted charged particles were well separated in the Si detectors (Fig. 1), while the  $\gamma$ -rays detected by MINIBALL, in coincidence with  $\alpha$  particles, clearly indicated the effective population of several states in Sr isotopes. A detailed analysis is ongoing.

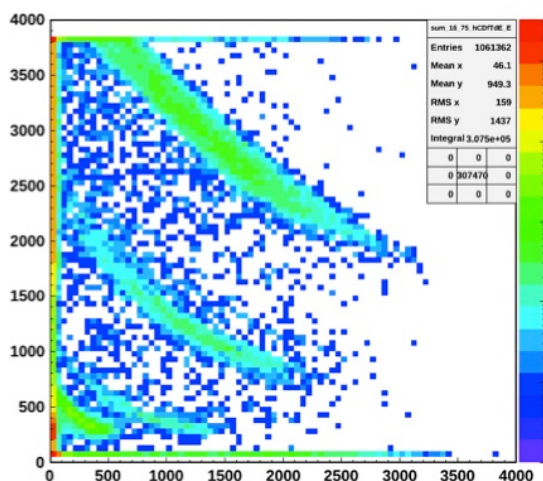


**Fig.1:** Event distribution detected in T-REX as a function of the  $\Delta E$  and  $E$  energies, measured in the CD and PAD-CD detectors, respectively. Structures corresponding to  $^7\text{Li}$  (top),  $\alpha$ ,  $t$  and protons (bottom) are clearly visible.

This experiment is the first example of the employment of  $(^7\text{Li}, X)$  cluster-transfer reaction for spectroscopy studies of nuclei far from stability. It provides a method which can be widely used in the future with the new generation of radioactive beams.

- [1] N. Marginean et al., PRC, 80(2009)021301.
- [2] J.L.Durell Proc.Int.Conf. On Spectroscopy of Heavy Nuclei, 1990.
- [3] F. K. Wohn et al., PRL, 51(1983)873.
- [4] G.D. Darcoulis et al., JPG: Nucl.Part. Phys. 23(1997)1191.
- [5] V. Bildstein et al., EPJ, A48(2012)85.

*Simone Bottoni for the IS536 collaboration*

## IS541: Beta-delayed protons from the decay of $^{11}\text{Be}$ ?

A decade ago IS374 attempted to find the rare beta-delayed proton decay process in the decay of  $^{11}\text{Be}$ . No positive identification could be found [1] and the final upper limit was of order a few times  $10^{-6}$ , which is the range of the most optimistic theoretical estimates that extend down to  $10^{-8}$ . Recent improvements in the yield of  $^{11}\text{Be}$  combined with enhancements in the sensitivity of the AMS (Accelerator Mass Spectrometry) technique used to detect the decay product  $^{10}\text{Be}$  should allow the limit to be reduced down to the  $10^{-8}$  range. We have therefore repeated the experiment.

The key ingredient for the experiment to succeed remains the selectivity of the HRS separator that is expected to be superior to what exists at other RIB facilities. The  $^{11}\text{Be}$  activity was found to decrease a factor  $10^3$  within 0.02 mass units, the distance to the possible contaminant  $^{11}\text{Li}$ . By blocking

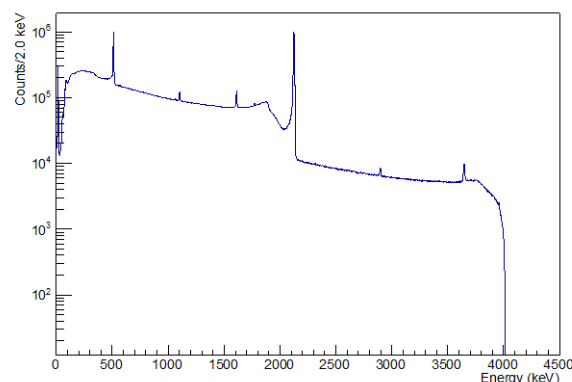


**Fig.1:** HPGe energy spectrum from the  $^{11}\text{Be}$  collection (only part of the data). The spectrum is dominated by the 2124 keV line in  $^{11}\text{Be}$ .

collection in the first 150 ms after proton impact a pure source could be obtained, as seen from the recorded gamma spectrum, figure 1, where apart from a 511 keV line only lines from the  $^{11}\text{Be}$  decay are seen. Roughly  $2 \cdot 10^{12}$   $^{11}\text{Be}$  atoms were collected.

The sample of  $^{11}\text{Be}$  as well as control samples are currently being prepared for AMS analysis at the VERA facility in Vienna. A final result is expected later this year.

1] M.J.G. Borge et al, J.Phys. G 40 (2013) 035109.

*K. Riisager (for the IS541 Collaboration)*

### IS543: Radioactive waste to probe exploding stars

The FERMI gamma ray satellite recently confirmed that core collapse supernovae are a source of cosmic rays [1]. A similarly impressive result from satellite-based observations of gamma rays may yet provide a measurement sensitive to the underlying core collapse mechanism itself. At present, this remains poorly understood, although significant improvements are being made [2]. Resolving this mystery would be a major achievement in understanding one of the Universe's most complex and extreme environments.

For such a measurement to be effective, improved knowledge of key nuclear reaction rates is required, the most important being  $^{44}\text{Ti}(\alpha, p)^{47}\text{V}$  [3]. The isotope  $^{44}\text{Ti}$  has a half-life of  $\sim 60$  yrs, with decays leading to 1.157 MeV gamma rays. In supernovae,  $^{44}\text{Ti}$  is produced in the region just above the collapsed core. The amount produced depends on the competing production and destruction reactions, of which the most uncertain is  $^{44}\text{Ti}(\alpha, p)^{47}\text{V}$ . Once produced, the amount of  $^{44}\text{Ti}$  ejected to more rarefied regions from which the gamma emission may be viewed by satellite depends on the (hydrodynamic) details of the explosion mechanism. With the nuclear physics adequately constrained, a satellite observation of gamma ray flux might be compared to alternative models of the

explosion mechanism and discrimination between them achieved.

One of the final experiments before the long shutdown, IS543 aimed to provide the first direct measurement of this key reaction at relevant energies. The beam was produced in a novel way. As part of the ERAWAST initiative [4], highly irradiated components from the SINQ spallation neutron source of the Paul Scherrer Institute were subjected to radiochemical separation, combining liquid-liquid extraction and ion-exchange chromatography. A sample of around 50 MBq atoms of  $^{44}\text{Ti}$  was obtained and dissolved in  $\text{HNO}_3$ . This sample was then poured, dried on a molybdenum foil, and shipped from PSI to CERN. It was inserted in a standard target container in the ISOLDE Class A target laboratory, connected to a VADIS FEBIAD ion source in the VD5 configuration, and equipped with a large  $\text{CF}_4$  gas leak to allow for the production of Ti beams as  $\text{TiFx}$  molecular ions [6]. The unit was then installed on the GPS Front End and a  $\text{TiF}_3^+$  molecular beam extracted. This was then dissociated during charge breeding in REX-ISOLDE before acceleration in a similar way to previously post-accelerated Sr beams.  $^{44}\text{Ti}^{13+}$  beams of around  $5 \times 10^5$  to  $5 \times 10^6$  pps, with no apparent isobaric contamination, were provided to the experimental apparatus for 4 days. Beams of 3.9 and 4.2 MeV (centre of mass) were provided.

The reaction target was a 2 cm long  $^4\text{He}$ -filled gas cell at a pressure of 50 Torr. Beam ions reached the target by traversing an entrance window formed of a 12 mm diameter, 6  $\mu\text{m}$  thick light-tight aluminium foil. Energy loss of the beam in this window meant the facility-delivered beam energy had to be significantly higher than the energy needed for the reaction being studied. An unwanted contribution from fusion-evaporation reactions of the beam and entrance window were avoided by

using as thin a window as possible, thus minimising the initial beam energy. By design, beam ions were stopped in the exit foil of the gas cell, preventing direct exposure of downstream silicon detectors to beam flux, and allowing a more robust 15  $\mu\text{m}$  window to be used. An additional benefit was that stopped ions became located at a well defined position, allowing a high-purity germanium detector, placed close by, to observe 1.157 MeV decay gamma rays. Counting of these allows an independent measurement of the accrued beam on target to be made.

Protons and alpha particles emanating from the gas cell were detected downstream in two 'S2' design segmented silicon detectors in a telescope configuration (70  $\mu\text{m}$  front detector, 1 mm back detector). Comparison of front detector signal ( $\Delta E$ ) against back detector ( $E$ ) allows particle identification. All heavier ions were stopped in the exit window.

Figure 1 shows a comparison of  $\Delta E$ - $E$  experimental data from runs with the gas cell filled to runs with the gas cell opened to the vacuum of the chamber ( $E_{\text{cm}}=4.2$  MeV). Also shown is a Monte Carlo simulation written before the experiment. In the simulation, three contributions were expected: protons from  $^{44}\text{Ti}(\alpha, p)^{47}\text{V}$  reactions in the gas (black symbols); protons from elastic scattering of the beam with hydrogen contamination residing on the surfaces of the gas cell windows (green symbols indicating contamination of the front of the entrance window; blue symbols from contamination of the back of the entrance window and/or the front of the back window); and alpha-particles from elastic scattering of the beam with the helium of the gas cell (red). The data also show each of these contributions with the alpha elastic scattering and the  $^{44}\text{Ti}(\alpha, p)^{47}\text{V}$  reactions being absent in the gas out run, as expected. Further analysis continues.

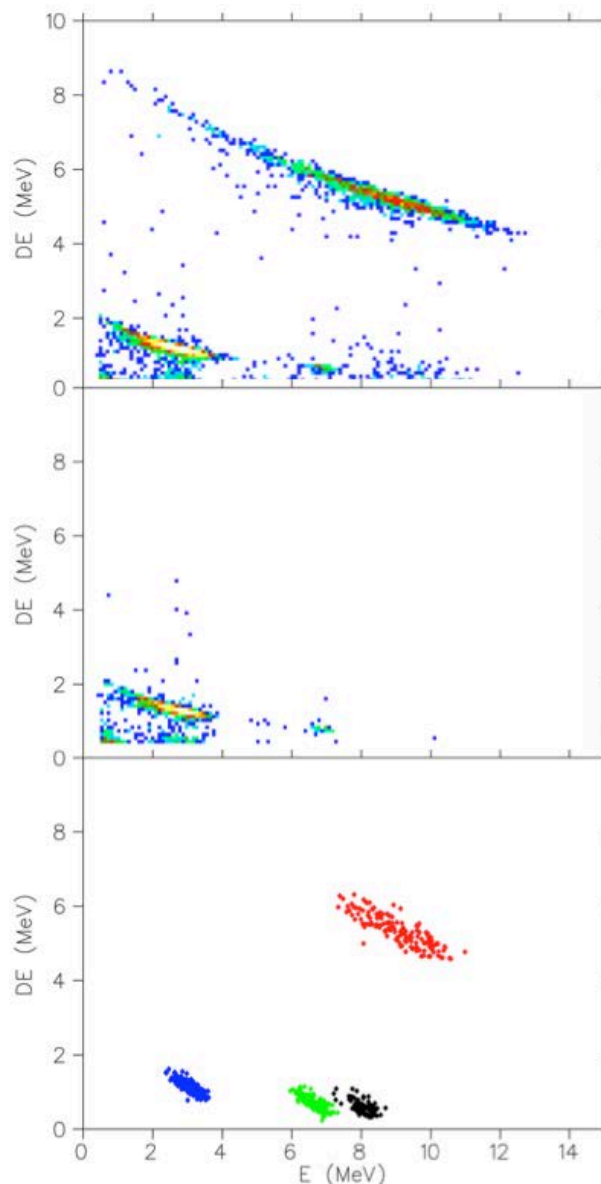


**Fig.1:** Plots of particle energy deposition in a  $\Delta E$ - $E$  telescope detector. Upper plot gas in; middle plot gas out; lower plot simulation. See text for details.

- [1] M Ackermann *et al.* Science 339 (2013)
- [2] H-T Janka *et al.* astro-ph:1211.1378v1.
- [3] G Magkotsios *et al.* Astrophys. J. Suppl. Ser 191 (2010) 66
- [4] <http://www.psi.ch/lch/erawast-i>
- [5] R Dressler *et al.* J. Phys. G: Nucl. Part. Phys. 39 (2012) 105201
- [6] L. Penescu *et al.*, Rev. Sci. Instr. 81(2), 02A906 (2010).

*Alex Murphy (for the IS543 Collaboration)*

## LOI83: Polarized beams at REX-ISOLDE

The possibility of controlling the spin orientation of an ensemble of nuclei can provide an important asset for many nuclear physics experiments. The nuclear spin polarization can provide specific information on the structure of the studied nuclear states, inaccessible by other means. In addition to nuclear structure studies the spin-orientation is of high interest for a number of disciplines such as solid-state physics, biophysics, chemistry etc. where the nuclear spin polarization could lead to many orders of magnitude higher experimental sensitivity.

Spin-oriented nuclear ensembles have been previously obtained by several ISOLDE experiments such as e.g. NICOLE (using Low-Temperature Nuclear Orientation), COLLAPS (using the Optical Pumping) or at the High-Voltage platform applying the Tilted Foils method [1,2]. In all of these the beam is either stopped in a catcher or with an extremely low energy that might hamper its further manipulations. Here we report on a project that applied the Tilted Foils approach on post-accelerated beams from REX-ISOLDE. The advantages of the Tilted Foils approach are: i) it is independent of the chemical nature of the probe nuclei; ii) it is relatively simple to be applied with a compact setup; and iii) the velocity of the ions after the TF setup could allow their further post-acceleration.

The first successful tests of the TF polarization after REX were performed in July 2012. A stack of 10 carbon foils ( $4 \mu\text{g}/\text{cm}^2$  each), preceded by a Mylar foil (used as energy degrader) were utilized to polarize a beam of  ${}^8\text{Li}$ , accelerated by REX to 300 keV/u. The level of nuclear polarization was monitored using the beta-NMR setup, installed at the second beam line. An NMR resonance was observed using

a frequency scan (see Fig. 1). From the observed amplitude of the resonance we could derive the level of nuclear polarization to be 3.6 (3) % or higher.

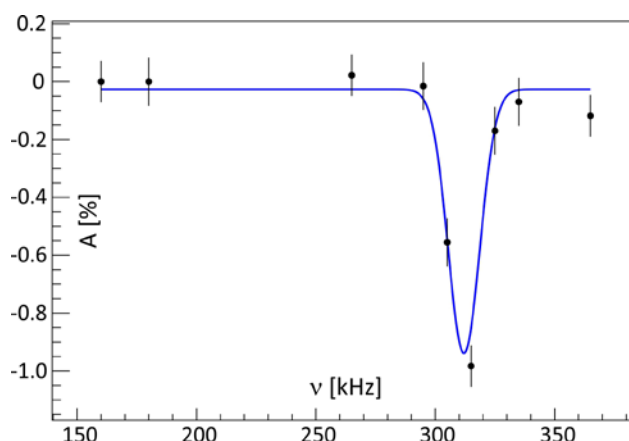


**Fig.1:** beta-NMR resonance observed for the 300 keV/u  ${}^8\text{Li}$  ions implanted in Pt host.

The polarization from this first test is very well in agreement with the results from similar measurements performed by Hirayama et al. [3] and demonstrates a clear reproducibility of the method. Some further studies of energy and/or charge-state dependence of the nuclear polarization using the TF method need to be done for its robust application on more exotic nuclei in different regions of the nuclear chart.

The success of the present tests could open up the possibility of post-accelerating spin-polarized beams at HIE-ISOLDE, which is presently under investigation.

[1] M. Lindroos *et al.*, Hyp. Int. 129, 109 (2000)

[2] L.T. Baby *et al.*, J. Phys. G 30, 519 (2004)

[3] Y. Hirayama *et al.*, Eur. Phys. Journ. A 48, 54 (2012)

*G. Georgiev for the beta-NMR – Tilted Foils polarization collaboration*

## LOI131: PAC study of the static and dynamic aspects of Cd and Hg atoms inside fullerene cage

The endofullerene compounds (atoms or cluster of atoms inside the fullerene cage) have applications in the areas of superconductivity, lasers, ferroelectric materials and nuclear medicines utilizing the behavior of atom(s) inside the cage [1]. The  $^{111m}\text{Cd}$  and  $^{199m}\text{Hg}$  beams from ISOLDE, CERN were implanted into  $\text{C}_{60}$  target ( $\sim 1\text{mg}/\text{cm}^2$ ) to produce respective endofullerene compounds. The coincidences for the 151-245 keV cascade of  $^{111m}\text{Cd}$  and 374-158 keV cascade of  $^{199m}\text{Hg}$  were used for TDPAC measurements on a six  $\text{LaBr}_3$  detector system coupled with digital electronics. The endofullerene compound was separated by filtration of the toluene

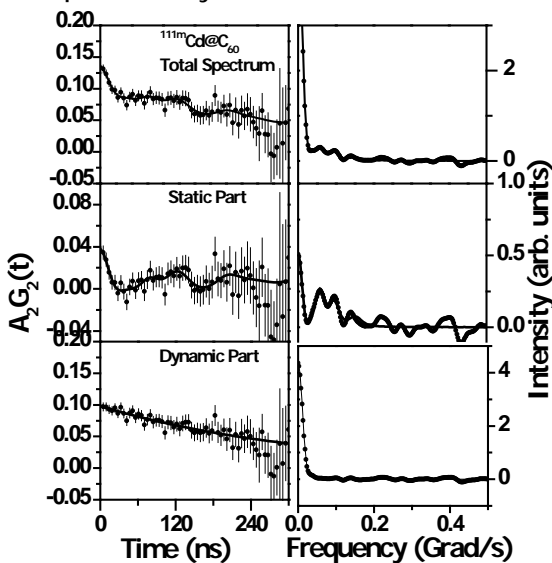


Fig.1: TDPAC spectrum for the  $^{111m}\text{Cd}@C_{60}$  endofullerene (left) and the corresponding Fourier spectrum (right).

solution of the implanted  $\text{C}_{60}$  target using micropore filter paper followed by solvent extraction with 6M HCl and was counted for TDPAC measurement. The results for the  $^{111m}\text{Cd}$  probe are shown in Fig.1.

The TDPAC results with the  $^{199m}\text{Hg}$  probe are shown in Fig2.

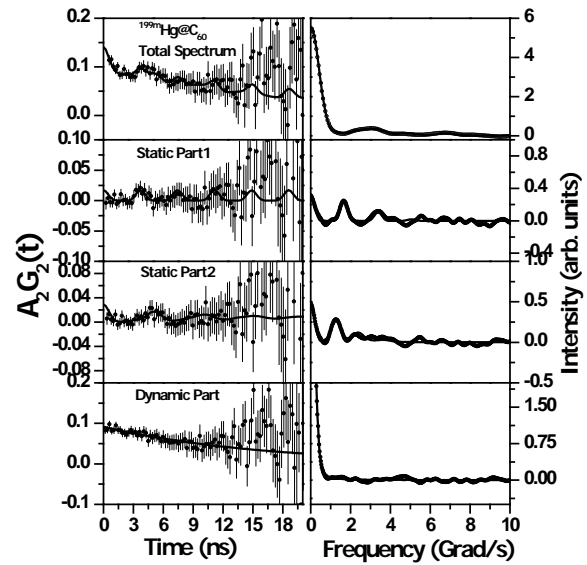


Fig.2: TDPAC spectrum for the  $^{199m}\text{Hg}@C_{60}$  endofullerene (left) and the corresponding Fourier spectrum (right).

The PAC parameters are tabulated in Table1.

Sample	$\omega_Q$ (Mrad/s)	$\eta$	$\delta$ (%)	Fast $\lambda$ ( $\text{ns}^{-1}$ )
$^{111m}\text{Cd}$	8.14(42)	0.42(9)	9.3(5.7)	0.003(3)
$^{199m}\text{Hg}$	281.6(16.9) 202.3(22.7)	0.1(1) 0.2(1)	0.01(2) 0.08(5)	0.06(9)

Table1: TDPAC parameters for two systems.

The results indicate that in case of both Cd and Hg atoms, there exists a static part along with a dynamic fraction due to a rapidly fluctuating electric field gradient. The static part might be attributed to a fraction of atoms externally trapped by fullerene-clusters formed during the implantation process. However, the dynamic part is attributed to the movement of the atoms inside the fullerene cage. Since  $\lambda$  is proportional to  $\omega_Q^2 \tau_c$  (correlation time) it follows that  $\tau_c$  for Hg is 1-2 orders of

magnitude smaller than that for Cd, i.e. Hg atoms remain loosely bound inside the fullerene cage due to its Inert-Pair effect.

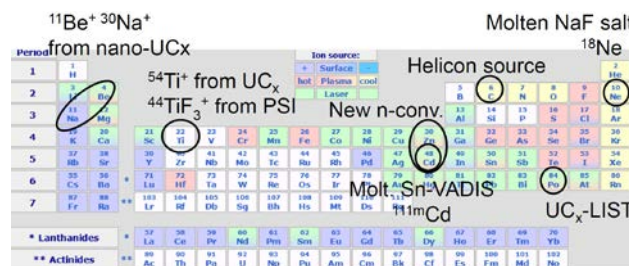
Reference:

[1] T. Braun (Ed.), Developments in Fullerene Science, Nuclear and Radiation Chemical Approaches to Fullerene Science, Vol. 1, Kluwer Academic Publishers, The Netherlands, 2000.

*S.K. Das, R. Guin, D. Banerjee, K. Johnston, P. Das, T. Butz, V. S. Amaral, J.G. Correia,, M. B. Barbosa.*

## Target and Ion Source Development (TISD):

2012 was a special year for the program of Target and Ion Source Development (TISD), since at the same time a longer operation and the forthcoming extended shut-down put some additional constraints on our activities. Yet last year witnessed a number of developments, and prepared the ground for some others. Activities were split between the 1<sup>st</sup> prototype design towards an improved neutron converter [1], the operation of a Helicon RF ion source for molecular CO<sup>+</sup> beams, coupling a VADIS ion source to a molten Sn target for Cd beams, operation of a molten salt target, the synthesis of UC<sub>x</sub> targets with nanostructures and the coupling of an improved LIST trap to a UC<sub>x</sub> target, Fig. 1. Many of these developments were reported at EMIS2012 in Matsue last year, and will be published in the proceedings.



Period	1	2	3	4	5	6	7
1	H	He					
2	Li	Be	B	C	N	O	F
3	Na	Mg	Al	Si	P	S	Cl
4	K	Ca	Sc	Ti	V	Cr	Mn
5	Rb	Sr	Y	Zr	Nb	Mo	Tc
6	Cs	Ba	La	Hf	Ta	W	Re
7	Fr	Ra	Ac	Rf	Sg	Bh	Hs

11Be<sup>+</sup> 30Na<sup>+</sup> from nano-UC<sub>x</sub>  
 54Ti<sup>+</sup> from UC<sub>x</sub>  
 44TiF<sub>3</sub><sup>+</sup> from PSI  
 Helicon source  
 Molten NaF salt  
 18Ne  
 New n-conv.  
 Molten Sn-VADIS  
 11mCd  
 UC<sub>x</sub>-LIST

*Fig. 1: Highlights of the beam developments at ISOLDE in 2012.*

Within the Beta Beams project [2], a molten salt target was proposed for the production of the required rates of <sup>18</sup>Ne [3,4]. Intermediate proton energy beams at 1 MW power are sent onto a circulating molten eutectic salt to produce and extract 10<sup>13</sup> <sup>18</sup>Ne/s. An important step towards its validation was achieved in 2012 at ISOLDE, within IS509, using a prototype static molten salt target unit.

The target material consisted of a mixture of NaF and LiF salts (39:61 molar ratio) with an eutectic point at 649°C. The choice of the material has been done taking into account  $^{18}\text{Ne}$  production yield as well as ensuring its stable and safe operation in a circulating loop. The prototyped unit, inspired by the standard ISOLDE target units, consisted of a hexacylindrical material container with a condensation chimney on top. Both target and chimney were constructed in a special Ni-rich alloy (Haynes 242), which is resistant to high-temperature corrosive fluoride environments and extremely hard to machine, requiring dedicated manufacturing approaches using resistant tools and water jet cutting. The target unit was further connected to a versatile arc discharge ion source (VADIS) [5] via a temperature controlled transfer line.

The validation of the prototype has been performed online at ISOLDE, where the release and production of low Z elements has been investigated. Particular attention has been devoted to the production and release of  $^{18}\text{Ne}$ , where a maximum yield of  $5.7 \cdot 10^4$  ions/ $\mu\text{C}$  has been obtained. This isotope was found to be released from the salt target within 100 ms, showing a fast release. Although the present yields are still below the best figures recorded at ISOLDE, an improvement of the intensity and release properties is expected with the use of a molten salt high power target loop exploiting MW proton beams.

Fig. 1 shows the conceptual layout of the proposed molten NaF:LiF high power target. Estimates suggest that intensities of 7 mA for a 160 MeV proton beam and a target dimensioned to dissipate 1.1 MW of deposited power, produce the required  $10^{13}$   $^{18}\text{Ne}/\text{s}$  for the Beta Beams project.

With 13 target units in 2012 uranium carbide continues to be the most requested

and versatile target material operated at ISOLDE. Although it is used in all major

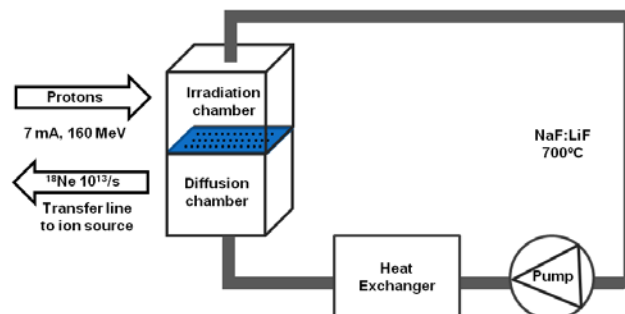


**Fig.2:** Layout of a molten NaF:LiF high power target loop for  $1\text{p}\cdot\mu\text{A}$   $^{18}\text{Ne}$  production for the Beta Beams [3,4].

ISOL facilities worldwide and is the reference material for future installations, such as HIE-ISOLDE, SPIRAL 2, SPES or ARIEL, little research and development have been performed due to its challenging properties concerning radio-toxicity and thermal instability. Despite this, thorough investigations of this material have now finally been launched covering both fundamental aspects of the material's structural and electronic properties and applied topics, already leading to the development of new target materials, an activity incorporated in the FP7-ENSAR Joint Research Activity ActILab, which is led by CERN [6].

State of the art X-ray absorption spectroscopy studies using a micro-focused synchrotron beam available at the Swiss Light Source (SLS) revealed numerous, yet unknown, properties [7]. Well defined  $\text{UC}_2$  samples of less than  $10^{-6}$   $\text{mm}^3$ , comprising just a few crystallographic grains, were prepared by vacuum nano-focused ion beam milling in a scanning electron microscope (SEM). Samples of this size are needed for two reasons. Firstly, performing the X-ray spectroscopy in transmission instead of reflection allows for more comprehensive theoretical modelling of the

collected data. Secondly, this technique shall be applied to irradiated ISOLDE UC<sub>x</sub> target material during this year, where only a volume as small as this would fall below the beam line's radioactivity limit of 100 LA. Fig. 3 shows a SEM picture of a sample cut superimposed with the false color map of the uranium distribution throughout the sample revealing the extended open porosity, essential for fast isotope release. By scanning the sample with the synchrotron spot in steps of 500 nm the distribution of all containing elements can be determined in this way down to a total atomic concentration of 10<sup>-9</sup>, together with the crystallographic structure by  $\mu$ XRD and the electronic structure by  $\mu$ EXAFS.

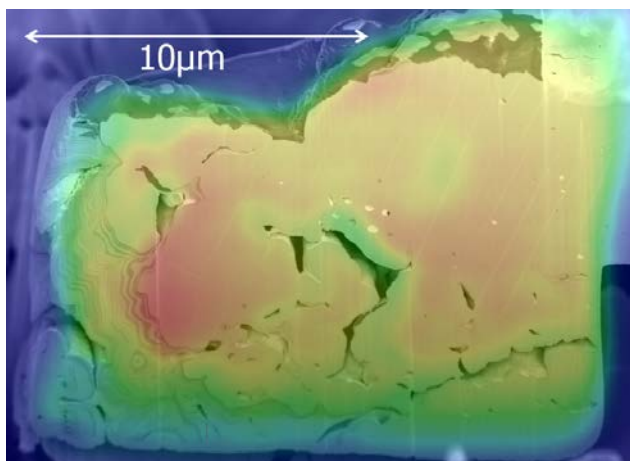


**Fig.3:**  $2 \cdot 10^4$  times magnification of a micrometric sample extracted from an ISOLDE UC<sub>2</sub>+C<sub>2</sub> target material, superimposed with the uranium elemental density, mapped by  $\mu$ XFS at the Swiss Light Source.

The observations made during these and other investigations finally led to the development of a new uranium carbide target material synthesized from nano-tailored uranium oxide and carbon powders, and tested within IS540, the last ISOLDE experiment before the long shutdown. This material was able to produce record yields of <sup>11</sup>Be and several n-rich Cs isotopes, while the material's structure seems to be widely preserved over time and temperature.

- [1] R. Luis et al. EPJ-A 48 (2012), 90.
- [2] P. Zuchelli, Phys Lett B 532 (2002), 166.
- [3] T. Stora, CERN Yellow Report, CERN-2010-003.
- [4] T.M. Mendonca, et al., J Phys: Conf Series 408 (2013), 012068.
- [5] L. Penescu, et al., Rev Sci Instrum 81 (2010), 02A906.
- [6] «Uranium carbide targets for radioactive ion beams: review and new developments» T. Stora 240th ACS meeting, Boston, 23rd Aug 2010. <http://www.nsl.msu.edu/~mantica/radio-frib/stora-acsboston.pdf>
- [7] «Uranium carbide target material investigations at ISOLDE/CERN», A. Gottberg, EURORIB'12, Abano Terme, 23rd May 2012. <http://agenda.infn.it/contributionDisplay.py?sessionId=8&contribId=81&confId=3946>

*A. Gottberg, T.M. Mendonca, T. Stora*

## How to obtain access to the ISOLDE hall

1. Register at the CERN Users office<sup>1</sup>. You need to bring
  - a. [Registration form](#) signed by your team leader or deputy<sup>2</sup>
  - b. [Home Institution Declaration](#)<sup>3</sup> signed by your institute's administration (HR).
  - c. Passport
2. Get your CERN access card in [Building 55](#)

With this registration procedure you become a **CERN user**<sup>4</sup>.

3. Follow the CERN basic safety course (levels 1 to 3):
  - a. If you have a CERN account, you can access the Safety Awareness course on-line at the web page <http://sir.cern.ch>, from your computer, inside or outside CERN.
  - b. If you have not activated your CERN account, there are some computers available for use without the need to log in on the first floor of building 55 (Your CERN badge will be needed in order to prove your identity).
4. Follow the online [RP course for Supervised Radiation](#). If you have not activated your CERN account see 3b.

5. Obtain a radiation dosimeter at the Dosimetry service, located in [Building 55](#)<sup>5</sup>. Two options exist:
  - a. Temporary dosimeter. Issued only once per calendar year for a maximum of 1 month.
  - b. Permanent dosimeter. A [medical certificate](#)<sup>6</sup>, valid for 24 months, is required. The permanent dosimeter needs to be readout monthly<sup>7</sup>.
6. Apply for access to ISOLDE hall using EDH:  
<https://edh.cern.ch/Document/ACRO>. This can be done by any member of your collaboration (typically the contact person) having an EDH account<sup>8</sup>.

Find more details at the [information about registration for Users](#) page.

New users are also requested to visit the ISOLDE User Support office while at CERN.  
Opening hours:  
Mon., Tues., Thurs., Fri. 08:30-12:30  
Mon. & Thurs. 13:30-15:30

---

<sup>1</sup> <http://cern.ch/ph-dep-UsersOffice> (Building 61, open 8:30-12:30 and 14:00-16:00, closed Wednesday morning).

<sup>2</sup> Make sure that the registration form is signed by your team leader before coming to CERN or that it can be signed by the team leader or deputy upon arrival.

<sup>3</sup> The Home Institution Declaration should not be signed by the person nominated as your team leader.

<sup>4</sup> The first registration as USER needs to be done personally, so please note the opening hours. If needed the extension of the registration can be delegated or performed on-line via EDH.

---

<sup>5</sup> <http://cern.ch/service-rp-dosimetry> (open *only in the mornings* 08:30 - 12:00).

<sup>6</sup> The medical certificate must be brought in person to the Dosimetry Service (either by the user or a representative)

<sup>7</sup> There are reader stations at the ISOLDE hall and the CERN main building. You can leave your *permanent dosimeter* in the rack outside the ISOLDE User Support office.

<sup>8</sup> Eventually you can contact Jenny or the Physics coordinator.

## Contact information

### ISOLDE User Support

Jenny Weterings

[Jennifer.Weterings@cern.ch](mailto:Jennifer.Weterings@cern.ch)

+41 22 767 5828

### Chair of the ISCC

Yorick Blumenfeld

[yorick@ipno.in2p3.fr](mailto:yorick@ipno.in2p3.fr)

+33 1 69 15 45 17

### Chair of the INTC

Klaus Blaum

[Klaus.Blaum@mpi-hd.mpg.de](mailto:Klaus.Blaum@mpi-hd.mpg.de)

+49 6221 516 851

### ISOLDE Physics Section Leader

Maria J.G. Borge

[mgb@cern.ch](mailto:mgb@cern.ch)

+41 22 767 5825

### ISOLDE Physics Coordinator

Magdalena Kowalska

[Magdalena.Kowalska@cern.ch](mailto:Magdalena.Kowalska@cern.ch)

+41 22 767 3809

### ISOLDE Technical Coordinator

Richard Catherall

[Richard.Catherall@cern.ch](mailto:Richard.Catherall@cern.ch)

+41 22 767 1741

### HIE-ISOLDE Project Leader

Yacine Kadi

[Yacine.Kadi@cern.ch](mailto:Yacine.Kadi@cern.ch)

+41 22 767 9569

More contact information at

<https://isolde.web.cern.ch/ISOLDE/default2.php?index=index/groupindex.htm&main=group/contacts.php> and at

<https://isolde.web.cern.ch/ISOLDE/default2.php?index=index/groupindex.htm&main=group/places.php>

